

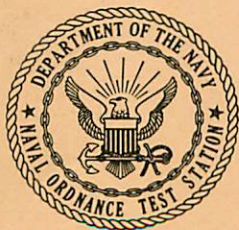
**FREE-SURFACE WATER-TUNNEL TESTS OF AN
UNCAMBERED BASE-VENTED PARABOLIC
HYDROFOIL OF ASPECT RATIO ONE**

by
Thomas G. Lang
and
Dorothy A. Daybell
Research Department

ABSTRACT. Results of water-tunnel tests on the base-vented hydrofoil model show that the lift and moment coefficients and the lift coefficient derivative are all essentially independent of ventilation number and are approximately equal to coefficients of uncambered airfoils having the same aspect ratio.

The drag coefficient agreed only partially with two-dimensional cavity drag theory. The maximum lift-to-drag ratio was 6.5 when fully vented and 2.4 when fully wetted.

Due to the reduced blockage of the Free Surface Water Tunnel at the California Institute of Technology, the minimum ventilation number (K) was 0.02 and the minimum air-flow rate coefficient (Q'_{cr}) providing full ventilation was 0.026 (rate increasing) and 0.013 (rate decreasing).



U. S. NAVAL ORDNANCE TEST STATION

China Lake, California

September 1962

U. S. NAVAL ORDNANCE TEST STATION

AN ACTIVITY OF THE BUREAU OF NAVAL WEAPONS

C. BLENMAN, JR., CAPT., USN
Commander

WM. B. McLEAN, Ph.D.
Technical Director

FOREWORD

This report is part of a series on vented hydrofoils published by the Naval Ordnance Test Station (NOTS). These studies concerning the exhaust of gas through hydrofoil surfaces provide information leading to new torpedo propeller designs and new methods of torpedo control.

An experimental study on a base-vented hydrofoil of parabolic cross-section was conducted in the Free Surface Water Tunnel at the California Institute of Technology from March through May 1961. The results and analysis, together with previous NOTS reports on vented hydrofoils, contribute toward the design of base-vented propeller blades having reduced susceptibility to cavitation.

The work was performed under Bureau of Naval Weapons Task Assignment RUTO-3E-000/216-1/009-01-003, problem assignment 401. Review for technical adequacy was performed by Henry Yerby and John Brooks of this Station.

T. E. PHIPPS, Head
Research Department

Released under
the authority of:

WM. B. McLEAN
Technical Director

NOTS Technical Publication 2942
NAVWEPS Report 7920

Published by Research Department
Manuscript 805/MS-5
Collation Cover, 20 leaves, abstract cards
First printing 255 numbered copies
Security classification UNCLASSIFIED

CONTENTS

Nomenclature	iv
Introduction	1
Experimental Apparatus and Procedure	1
Description of the Model	1
Water Tunnel	1
Instrumentation	3
Test Procedure	7
Data Reduction	8
Strut Pressure Interference	9
Results and Analysis	10
Description of the Flow	10
Lift	16
Drag	16
Moment Coefficient	21
Air-Flow Rate	22
Ventilation Number	24
Lift-to-Drag Ratio	24
Conclusions	26
Appendixes:	
A. Corrections Applied to the Force Data	27
B. Air-Flow Data Reduction	31
References	32

NOMENCLATURE

- A Planform area of hydrofoil (bc), ft²
- A_b Base area of hydrofoil (bt), ft²
- AR Aspect ratio of hydrofoil (b/c)
- b Span of hydrofoil, ft
- c Chord of hydrofoil, ft
- C_D Drag coefficient (D/q_∞A)
- C_d The portion of C_D that varies with α: C_d = C_D - C_D(C_L = 0)
- C_{Dm} Measured drag coefficient, parallel to tunnel center line
- C_{DJ} Air jet drag coefficient
- C_{Ds} Strut drag coefficient
- C_L Lift coefficient (L/q_∞A)
- C_{Lm} Measured lift coefficient, perpendicular to tunnel center line
- C_{La} Lift coefficient derivative (dC_L/da), per radian
- C_M Pitching-moment coefficient (about quarter-chord point)(M/q_∞Ac)
- C_{Ma} Pitching-moment coefficient derivative (dC_M/da), per radian
- d Depth of model center line below undisturbed free surface, ft
- D Drag, lb
- D' Drag coefficient (D/q_∞A_b)
- K Ventilation number (P_∞ - P_c)/q_∞
- L Lift, lb
- L/D Lift-to-drag ratio

- P_l Pressure in high-pressure air-supply line, lb/ft²
- P_c Cavity or base pressure, lb/ft²
- P_s Standard pressure for air-flow meter calibration, 2,120 lb/ft²
- P_∞ Free-stream static pressure, lb/ft²
- q_∞ Free-stream dynamic pressure ($1/2\rho V_\infty^2$), lb/ft²
- Q Air-flow rate at free-stream static pressure as derived in Appendix B, ft³/sec $\left(Q_m \frac{P_l}{P_\infty} \sqrt{\frac{P_s}{P_l}} \right)$
- Q' Air-flow rate coefficient ($Q/V_\infty A_b$)
- Q'_{cr} Value of Q' at which model first becomes fully vented
- Q_l Air-flow rate in high-pressure air-supply line, ft³/sec
- Q_m Air-flow meter reading, ft³/sec
- t Base thickness of hydrofoil, ft
- V Velocity
- V_∞ Free-stream velocity, ft/sec
- x Distance from leading edge along chord of hydrofoil, ft
- y Distance perpendicular to chord of hydrofoil, ft
- α Corrected angle of attack, radians, unless otherwise stated ($\alpha = \alpha_{meas} - \alpha_0$)
- α_0 Angle of attack (uncorrected) at which the lift coefficient (corrected for tare and buoyancy) was zero, radians
- α_{meas} Measured angle of attack (angle between model center line and tunnel center line), radians
- ρ Mass density of water, slug/ft³
- θ Angle between free-stream flow direction and tunnel center line, radians

INTRODUCTION

The purpose of this experimental program was to investigate further a relatively new type of hydrofoil--the base-vented hydrofoil (Ref. 1). Base-vented hydrofoils might be used as stabilizing and control surfaces, or as the blades of propellers and pumps, or as the lifting surfaces of hydrofoil-supported craft. An earlier series of experiments on vented hydrofoils (Ref. 2 and 3) was conducted by the Naval Ordnance Test Station during 1958 and 1959 in the High-Speed Water Tunnel (HSWT) at the California Institute of Technology (CIT). Although the force measurements were in fair agreement with the recent theory of Ref. 4 and 5, various types of tunnel-wall interference prevented complete agreement. The cavity shape was distorted by blockage effects, and the cavity pressure could not be increased sufficiently close to the tunnel static pressure. Also, it was not known whether the wall interference affected the minimum value of the air-flow rate required to first create a long steady air cavity.

The new test series was conducted to investigate more fully the gas ventilation rate, the effects of tunnel wall and strut interference, and to obtain new data on a slightly different hydrofoil shape. This series of tests was conducted in the Free Surface Water Tunnel (FSWT) at CIT where the wall interference effects are theoretically very small.

EXPERIMENTAL APPARATUS AND PROCEDURE

DESCRIPTION OF THE MODEL

The hydrofoil used for this experiment was uncambered and had a parabolic cross section with a thickness-to-chord ratio of 0.15, a 4-inch chord, and a 4-inch span (Fig. 1 and 2). The model was vented by exhausting air through the base of the model. The cavity pressure was measured at the single hole in the center of the base.

WATER TUNNEL

These experiments were carried out in the FSWT at CIT (Ref. 6). The tunnel is of the closed-circuit type and is capable of velocities up to 26 ft/sec. The working section is 7.5 feet long with a rectangular cross section of 1.6-foot width and a nominal water depth of 1.65 feet.

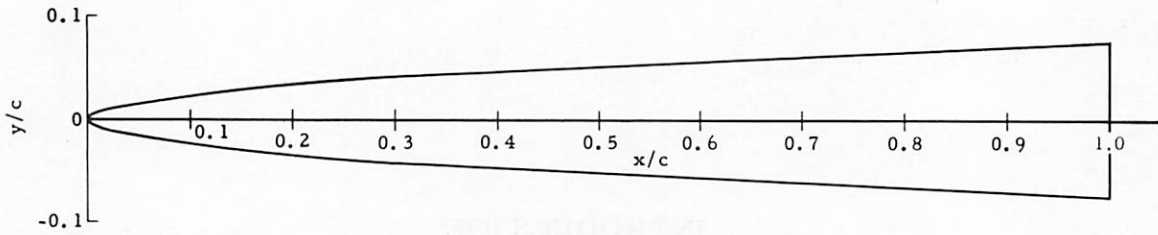


FIG. 1. Cross Section of Parabolic Hydrofoil.

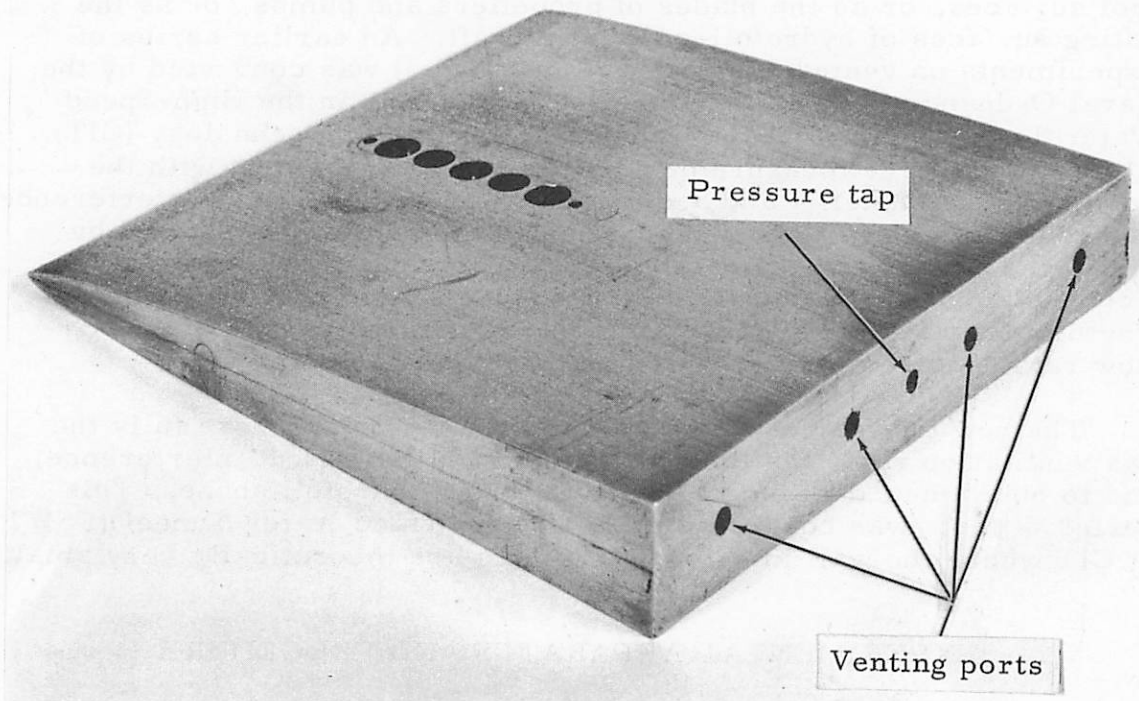


FIG. 2. Model Showing Venting Ports and Pressure Tap.

INSTRUMENTATION

Two force-balance and strut combinations were used for this experiment. The first combination consisted of the CIT three-component mechanical force balance (Ref. 7), and a shielded strut. Figures 3 and 4 show the strut mounted on the balance, with and without the shield. The strut shield had a streamlined cross section (Convair shape No. E451402, Rev. 1) with a 4-inch chord and 0.81-inch maximum thickness. The exposed (lower) part of the strut that supported the model had a biconvex cross section with a 1.75-inch chord, a thickness of 0.210 inch, and a height of approximately 1.75 inches. This strut was pivoted to an internal brace at a point 2.4 inches above the model center line to permit changes in the angle of attack. Polyethylene tubing was used to duct the air through the strut shield to the support strut. A duct through the support strut intersected a manifold inside the model that led to the four exhaust ports. A similar duct and tubing connected the base pressure tap to the manometer. Figure 5 is a schematic of the air-flow and cavity-pressure instrumentation for the shielded strut.

The second force-balance and strut combination consisted of a six-component strain-gage force-balance¹ and a streamlined unshielded strut² (Fig. 6). The strut had an NACA 16-006 cross section (Ref. 8) with a chord of 2.25 inches. It was swept back 9 degrees from the vertical when the model angle of attack was zero. A pivot at the upper end of the strut permitted changes in the angle of attack of the model. It was not possible to supply air to the model through the thin unshielded strut. A separate strut downstream of the model (Fig. 7) supported an air-supply tube and a cavity-pressure probe, both of which projected forward into the downstream end of the cavity. With the separate air supply, it was not possible to obtain cavities at low air-flow rates. The downstream pressure tap did not permit the measurement of base pressures when the model was fully wetted. Figure 8 is a schematic of the air-flow and cavity-pressure instrumentation for the unshielded strut.

Air-cavity pressures were measured by a water manometer open to the atmosphere at the top. The line from the manometer to the pressure tap at the bottom of the model was kept clear of water by continuously bleeding a small amount of air through it. This measurement is accurate to within ± 0.01 foot of water. The water velocity was obtained from the total head pressure in the tunnel upstream of the contraction nozzle. The accuracy was ± 0.15 ft/sec. The air-flow rate

¹ Mark II model, manufactured by the Task Corp., Anaheim, Calif.

² The unshielded strut and the readout equipment for the strain-gage balance were loaned to NOTS by the Aero-Space Division of the Boeing Airplane Co.

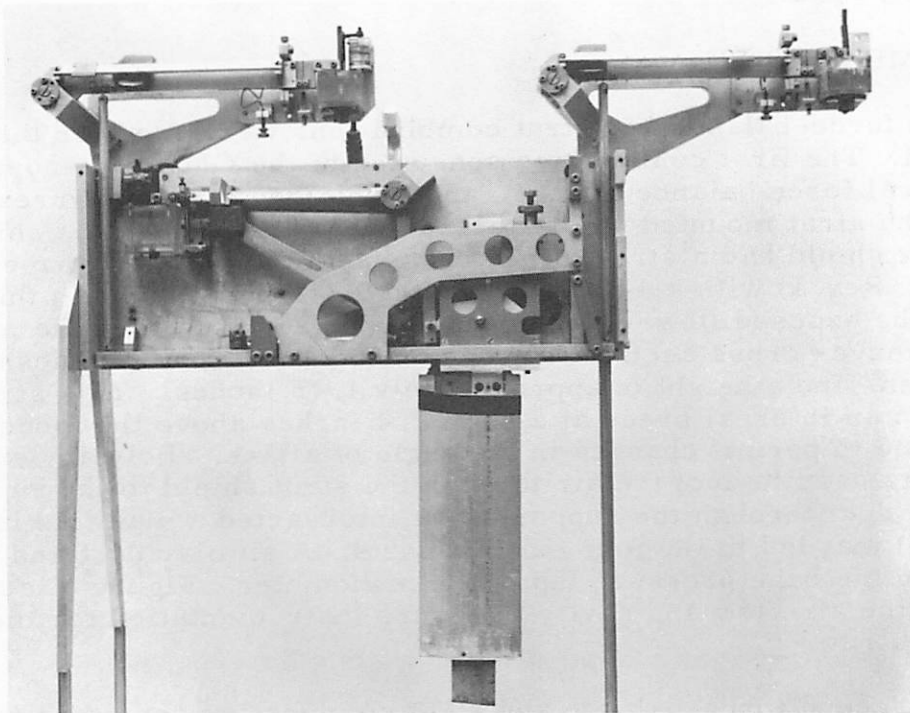


FIG. 3. Three-Component Mechanical Balance With Shielded Strut.

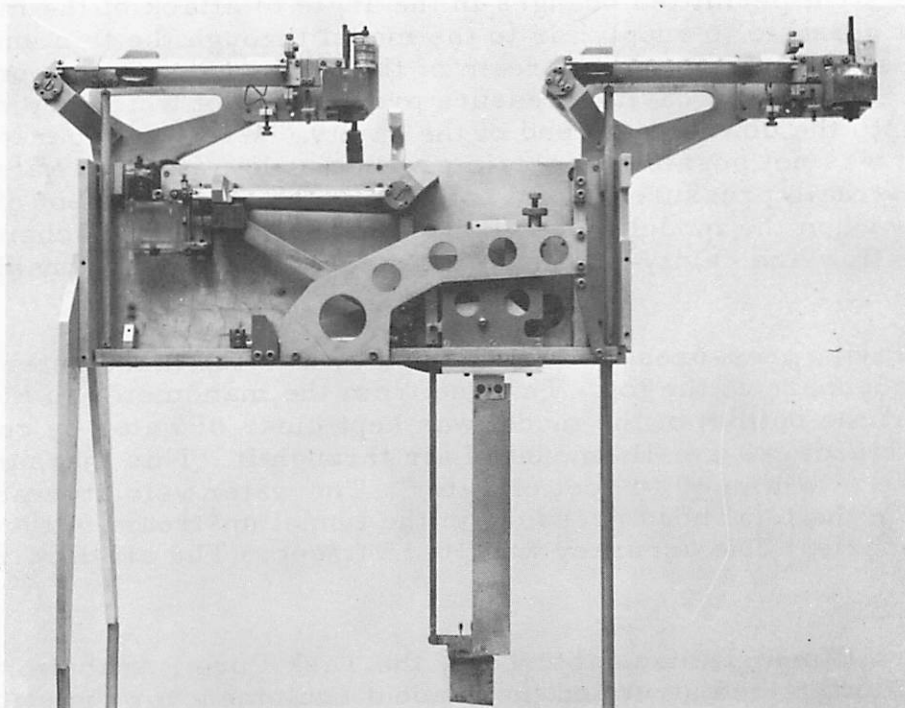


FIG. 4. Three-Component Mechanical Balance and Strut With Shield Removed.

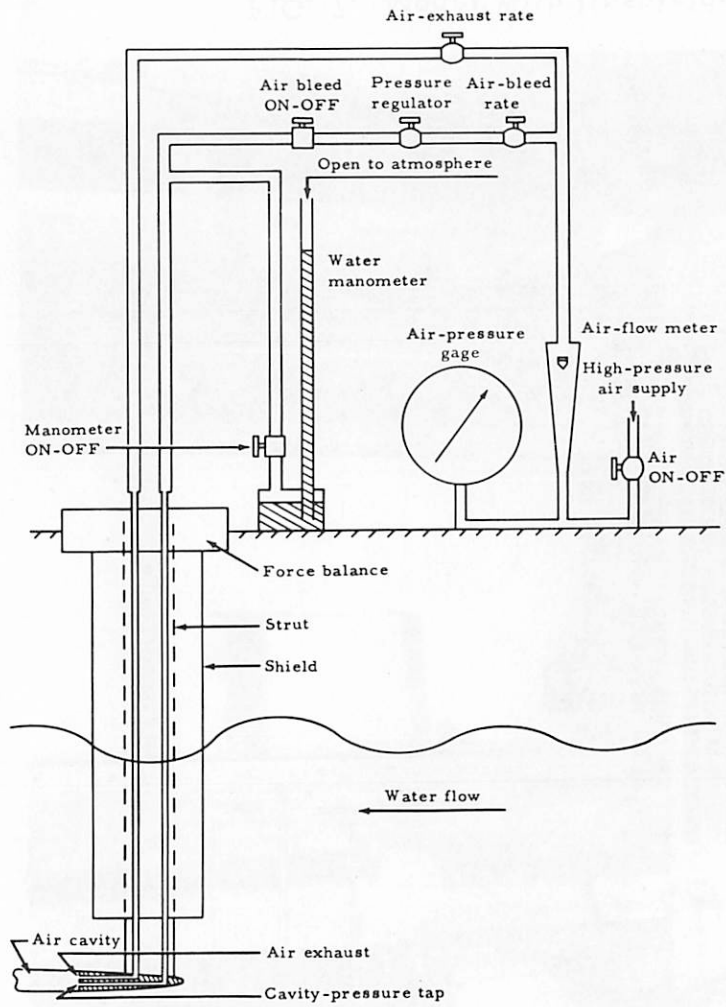


FIG. 5. Test Setup; Shielded Strut Support.

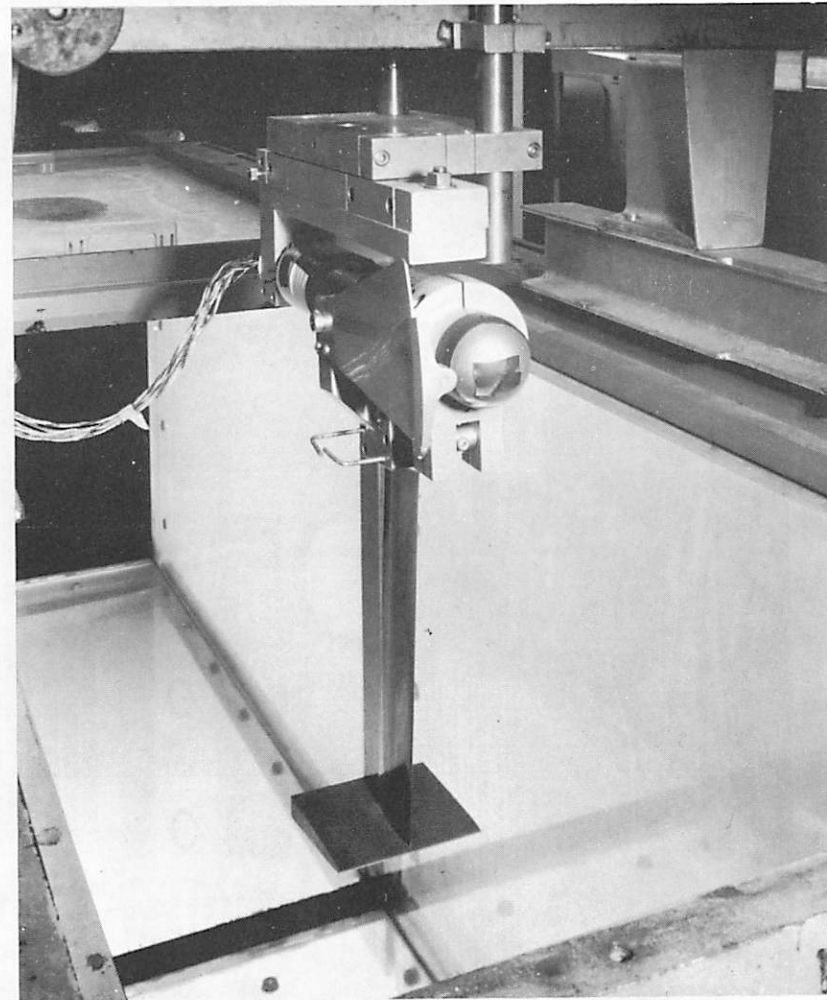


FIG. 6. Strain Gage Balance, Unshielded Strut and Model Mounted in Tunnel.

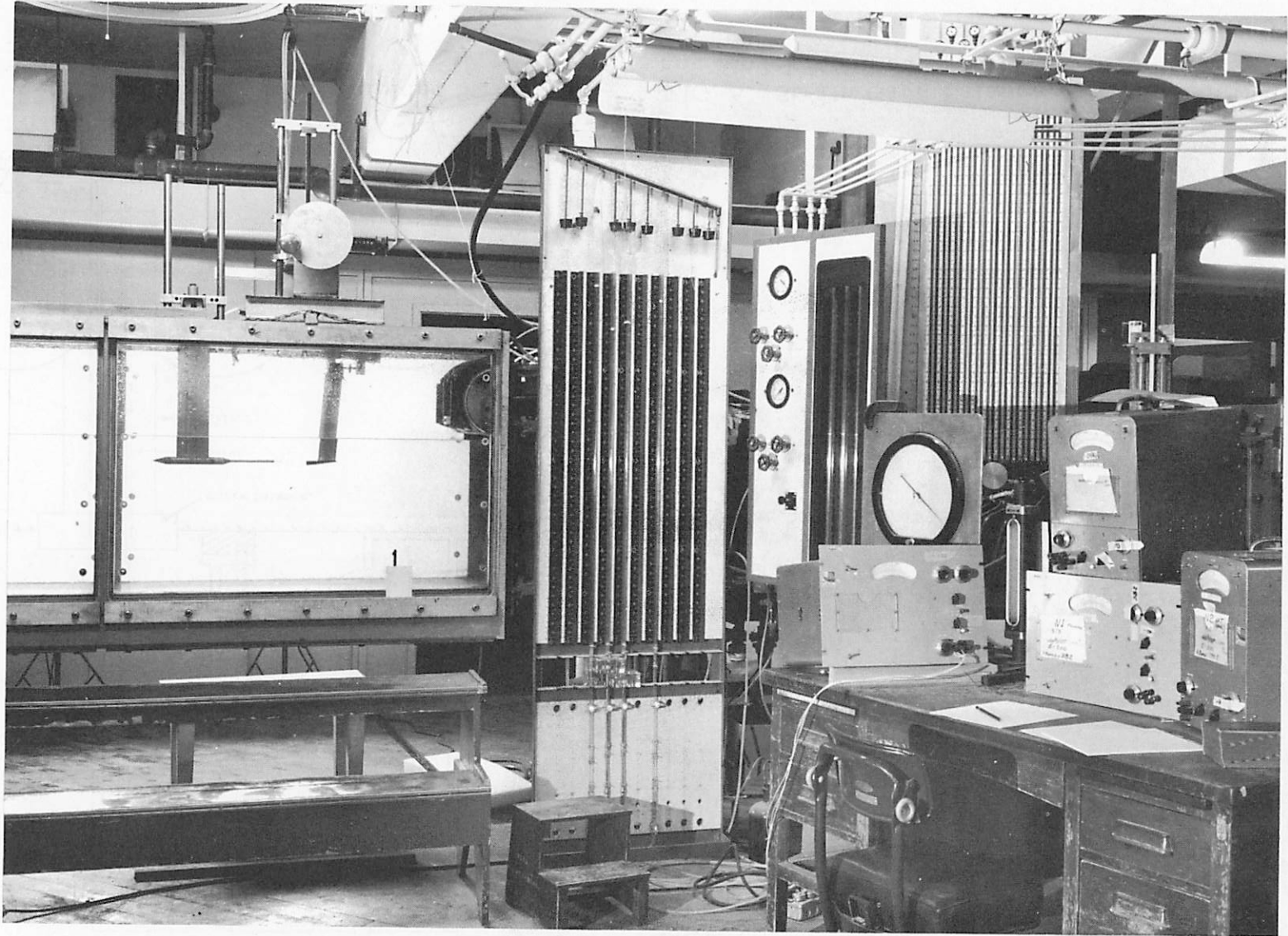


FIG. 7. Model With Unshielded Strut Mounted in Tunnel With Air-Supply Sting Positioned Behind.

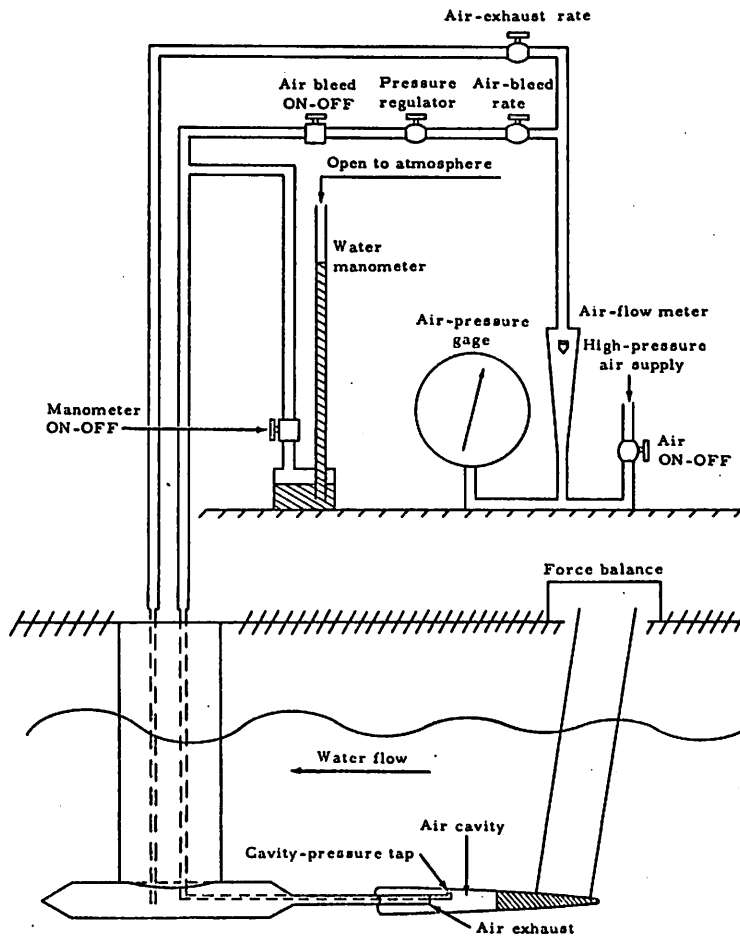


FIG. 8. Test Setup; Unshielded Strut Support.

was measured with a float-type flowmeter and the air pressure with a precision dial gage. The accuracy of these measurements is within 5%.

Photographs were taken of side and bottom views of the model at typical data points. "Streak" photographs were obtained by using an 0.5-second exposure time with photo-flood lamps; "flash" photographs were obtained by high-speed flash lamps with a duration of 10 micro-seconds.

TEST PROCEDURE

Force-balance zeroes were obtained with the model set at the desired angle of attack and placed above the water surface. The tunnel was then brought up to speed and the model lowered to the test depth. The air-flow rate was adjusted by either increasing or decreasing the flow rate, depending upon the test. After reading the forces, velocity, air-flow rate, air pressure and cavity pressure, the air-flow rate was

changed and new readings were taken. At the end of a sequence of data points, the model was raised from the water and the zeroes were read. The process was repeated for other angles of attack.

Runs were made with the shielded strut at a water velocity of 20 ft/sec and a model depth of two chords. Runs with the strain-gage balance were made at 20 ft/sec with model depths of two chords and one quarter chord, and at 25 ft/sec with a model depth of one chord.

DATA REDUCTION

The data were reduced to the following dimensionless coefficients:

Lift coefficient $C_L = \frac{\text{lift}}{q_{\infty}A}$

Drag coefficients $C_D = \frac{\text{drag}}{q_{\infty}A}$

$D' = \frac{\text{drag}}{q_{\infty}A_b}$

Pitching moment coefficient
(about quarter-chord point) . . . $C_M = \frac{\text{moment}}{q_{\infty}A_c}$

Ventilation number $K = \frac{P_{\infty} - P_c}{q_{\infty}}$

Air-flow rate coefficient $Q' = \frac{\text{air-flow rate}}{V_{\infty}A_b}$

Lift-to-drag ratio L/D

The force data were reduced as a function of system geometry, and corrected (Appendix A) for buoyancy effects and for all the strut tare effects except pressure interference.

All the lift curve data were shifted so that the lift was zero at zero angle of attack. The drag and moment data were plotted, using the shifted angle of attack. The shift in angle of attack for zero lift was believed to be due primarily to strut pressure interference, and secondarily to tunnel water-flow deviation and to change in zero-lift angle caused by the nearness of the water surface. The measured angle of zero lift was -1.5 degrees at a depth of two chords for the fully wetted model with the shielded strut, and -0.65, -0.40, and 0.0 degrees with the unshielded strut at respective depths of two, one, and one quarter chords. The contribution to these values of tunnel water-flow deviation

was found to be 0.25 degree at a depth of two chords, then tapering to zero at the surface.³

The moment data measured with the mechanical balance is not accurate since the data reduction process involves the difference of two large numbers, including the correction of moment due to drag force. No moment data were measured with the strain-gage balance.

STRUT PRESSURE INTERFERENCE

The presence of the support struts significantly influenced the hydrodynamic forces exerted on the model. This influence resulted from a deviation in pressure distribution and flow direction near the model. The thick shielded strut produced a much greater interference than the thin unshielded strut.

After the test program was completed, a special study to measure the strut-pressure interference was conducted by CIT.⁴ The model was mounted from the mechanical balance using the thin unshielded strut. The force readings duplicated the previous measurements that were obtained with the strain-gage balance. A thick strut, similar in size to the shield used with the shielded strut, was then placed near the model but offset slightly outboard of the center line. The resulting change in the model forces was almost identical to the differences in the force measurements previously obtained between the two struts. No tares were taken to correct the data for strut-pressure interference. If such a tare correction were obtained by mounting an image strut under the model, it would not be sufficiently accurate since the image system would not duplicate the influence of the water surface.

The effect on lift of the strut interference was accounted for by the arbitrary shift in zero-lift angle to zero degrees. Little effect of strut interference is expected on $C_{L\alpha}$ or CM_{α} since it is not likely to be significantly changed by small variations in angle of attack.

Although the model drag was greatly affected by the shielded strut, it was not measurably affected by the unshielded strut because any change in model drag due to pressure interference would have been canceled by an equal and opposite change in strut drag. Consequently, the major tare corrections for the unshielded strut are frictional drag and buoyancy.

The data in this report are labeled to distinguish between those taken using the shielded strut and those taken using the unshielded

³ Measured by T. Kiceniuk at CIT.

⁴ Unpublished internal CIT report, Experimental Memo E-118.2, by J. Brentjes.

strut. The only data with the shielded strut that have not been corrected are the drag data. It is believed that the data using the unshielded strut have been corrected for all major tares. The arbitrary shift in zero-lift angle to correct for pressure interference prevents analysis of the effect of the water surface on lift.

RESULTS AND ANALYSIS

The results are plotted in Fig. 17 through 26, and a summary of the results is presented in Table 1.

DESCRIPTION OF THE FLOW

The vortex pattern in the wake behind the blunt-based model is shown in Fig. 9. A small amount of air was exhausted through the trailing edge of the model to permit the vortices to be seen. The vortex pattern (Fig. 9) suddenly disappeared when the air-flow rate was increased to a certain critical value, Q'_{cr} . At this time, the hydrofoil was called fully vented since the cavity became a single clearly defined shape (Fig. 10), and remained so as the air-flow rate was further increased. Some hysteresis (Ref. 2 and 3) was again noticed, since the cavity retained its singular shape and did not return to the vortex pattern until the air-flow rate was reduced to a value less than Q'_{cr} . The upper trail of bubbles seen in these photographs has no relationship to the venting of the model; it is merely air that has been drawn down from the water surface through the inside of the strut shield and is escaping through the lower end.

In Fig. 11, where the angle of attack is 7.5 degrees, the air cavity behind the model consists of three parts: the central cavity and the two tip-vortex cavities. At zero angle of attack, only a single individual cavity is seen. At an angle of attack of -4.5 degrees (Fig. 12 and 13), the tip vortices are reversed and appear on the lower side of the central cavity. The bottom view (Fig. 13) shows that the central cavity and the tip vortex cavities terminate at different downstream locations.

It is important to note that the air cavity did not spring ahead of the trailing edge unless debris collected at the leading edge (Fig. 14). Except for this phenomenon, the Kutta condition at the trailing edge was apparently satisfied throughout the entire test range. Cavitation did not occur at any time during this test series.

The unshielded strut and model, together with the air-supply sting, are shown in Fig. 15. The subcritical air-flow rates that correspond to the trailing-vortex type of air cavity could not be maintained using the sting air supply. Consequently, all data obtained using the unshielded

TABLE 1. Results of Tests in Free Surface Water Tunnel

All results refer to tests of the uncambered base-vented hydrofoil model having a parabolic cross section with a thickness-to-chord of 0.15 and an aspect ratio of 1.0.

Item	Strut ^a	Value	Fig. No.	Comments
Lift Coefficient				
C_{L_a} (d = 2c, fully wetted)	S	1.64	17	Theory = 1.48 (d = ∞)
C_{L_a} (d = 2c, fully vented)	S	1.70	17	Theory = 1.48 (d = ∞)
C_{L_a} (d = 2c, fully wetted or vented)	U	1.75	18	Theory = 1.48 (d = ∞)
C_{L_a} (d = 1c, fully wetted or vented)	U	1.68	18	
C_{L_a} (d = 1/4c, fully wetted)	U	1.25	18	
Drag Coefficient				
C_d (α = 0°, K = 0.23, fully wetted)	S	0.0470	20	Theory = 0.035 (cav. drag)
C_d (α = 0°, K ≈ 0.23, fully wetted)	U	0.0515	19	Theory = 0.035 (cav. drag)
C_d (α = 0°, K = 0.025, fully vented)	S	0.0045	20	Theory = 0.0096 (cav. drag)
C_d (α = 0°, K = 0.025, fully vented)	U	0.0140	19	Theory = 0.0096 (cav. drag)
dD'/dK (α ≈ 0°, K > 0.02)	S	1.35	22	Theory = 1.0 for K > 0.15 and 0.5 for K = 0.04
dD'/dK (α ≈ 0°, K > 0.02)	U	1.26	21	HSWT ^b (exper.) = 1.08 for K > 0.06
$\pi AR C_d/C_L^2$ (0.23 < K < 0.35, fully wetted)	S	2.50	20	K increases as /α/>0
$\pi AR C_d/C_L^2$ (0.23 < K < 0.35, fully wetted)	U	2.86	19	K increases as /α/>0
$\pi AR C_d/C_L^2$ (K ≈ 0.03, fully vented)	S	1.92	20	Theoretical induced drag ≈ 1.0
$\pi AR C_d/C_L^2$ (K ≈ 0.03, fully vented)	U	1.37	19	Theoretical induced drag ≈ 1.0
Moment Coefficient				
C_M (α = 0, 0.02 < K < 0.20 fully vented)	S	-0.010 to +0.002	23	Theory = 0.00
CP (vented)	S	0.20	23	Theory = 0.17
CP (fully wetted, α < 1.5°)	S	0.20	23	Theory = 0.17
CP (fully wetted, α > 1.5°)	S	0.29	23	Theory = 0.17
Air-Flow Rate				
Q'cr (α = 0°, air flow increasing)	S	0.026	24	HSWT ^b = 0.07 (AR = 1.44 and AR = ∞)
Q'cr (α = 0°, air flow reducing)	S	0.013	24	HSWT = 0.03 (AR = 1.44)
dK/dQ' (-4.5 < α < 7.5°, fully vented)	S	-0.067	24	HSWT = -0.016 (AR = ∞)
Q'min (ventilation by aux. sting, flow reducing)	U	0.010 to 0.020	24	
Ventilation Number				
Kmin (0° < α < 2.5°, 0.10 < Q' < 0.20)	S	0.020 to 0.025	24	HSWT = 0.15 (AR = ∞) = 0.06 (AR = 1.44)
Kmin (-2° < α < 4°, 0.10 < Q' < 0.20)	U	0.020 to 0.025	24	
dC _L /dK (-4.5° < α < 7.5°)	S	≈ 0	26	HSWT ≈ 0 (AR = ∞)
dC _m /dK (-4.5° < α < 7.5°)	S	≈ 0	23	HSWT = -0.06 (AR = ∞) ≈ 0 (AR = 1.44)
Lift-to-Drag Ratio				
(L/D) _{max} (AR = 1.0, d = 2c, α = 7°, fully wetted)	U	2.4	27	HSWT = 4.0 (AR = 1.44)
(L/D) _{max} (AR = 1.0, d = 2c, α = 6°, fully vented)	U	6.5	27	HSWT = 8.5 (AR = 1.44)

^a S refers to shielded strut support and U to unshielded strut support.

^b All HSWT data were taken on a cambered parabolic hydrofoil with design lift coefficient at α = 0° (C_{l_d}) = 0.40, t/c = 0.15, and AR = 1.44 and infinity (Ref. 3).

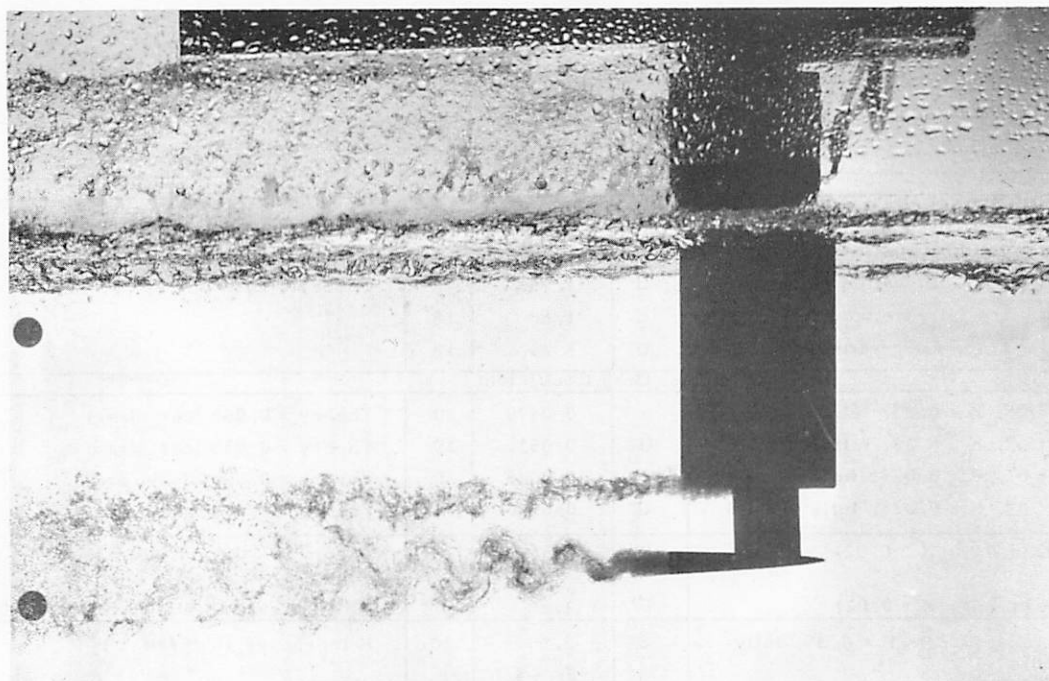


FIG. 9. Model With Shielded Strut, Subcritical Air-Flow Rate.

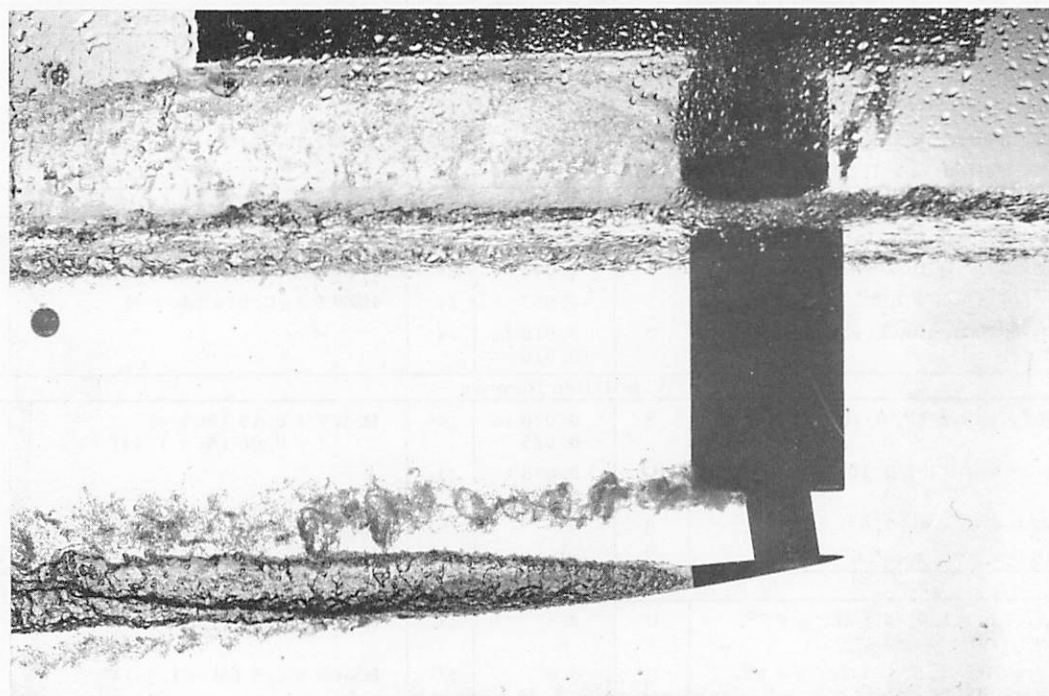


FIG. 10. Model Fully Vented, $Q' = 0.12$, $\alpha = 7.5$ deg.

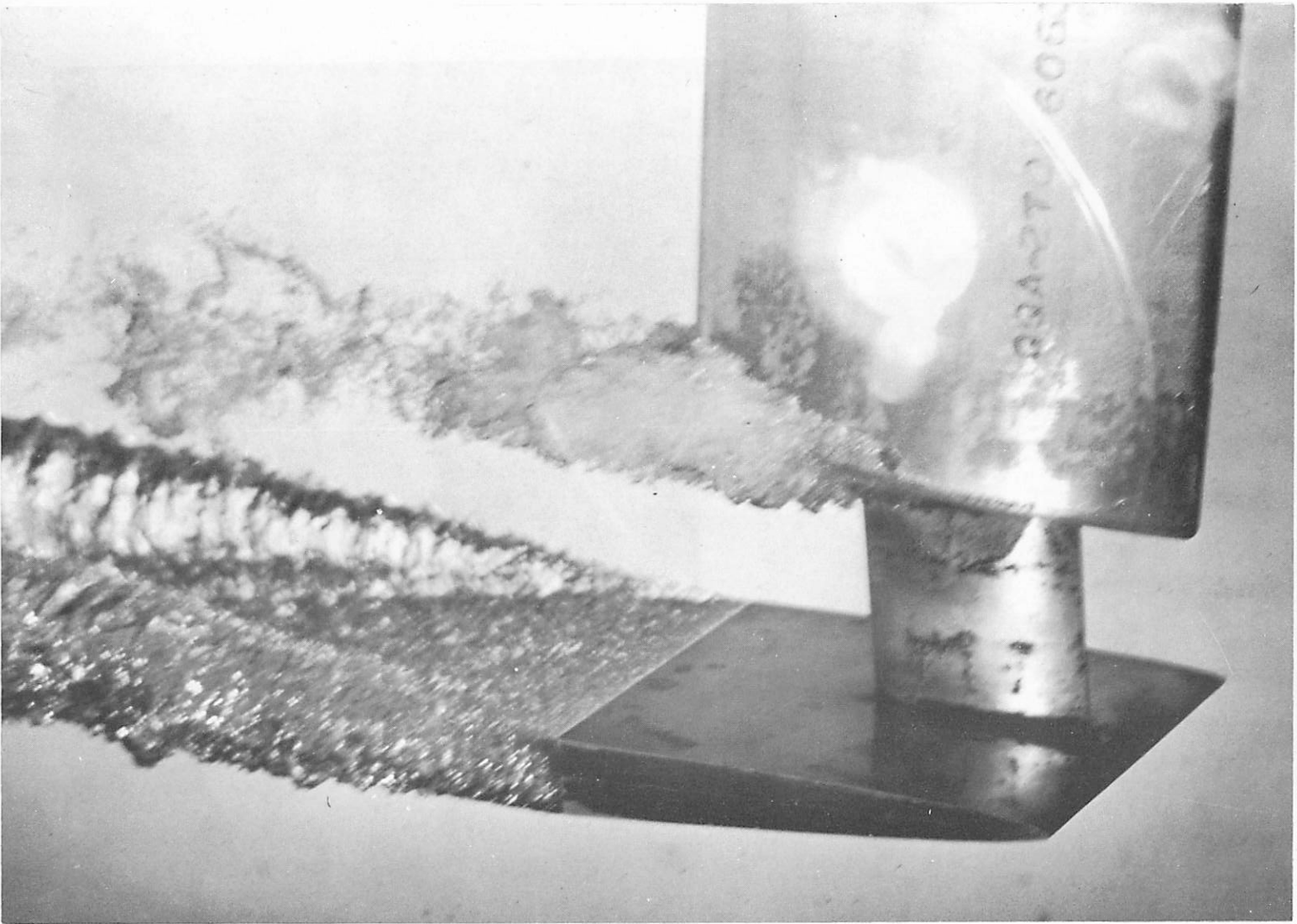


FIG. 11. Closeup of Model, $Q' = 0.12$, $\alpha = 7.5$ deg.

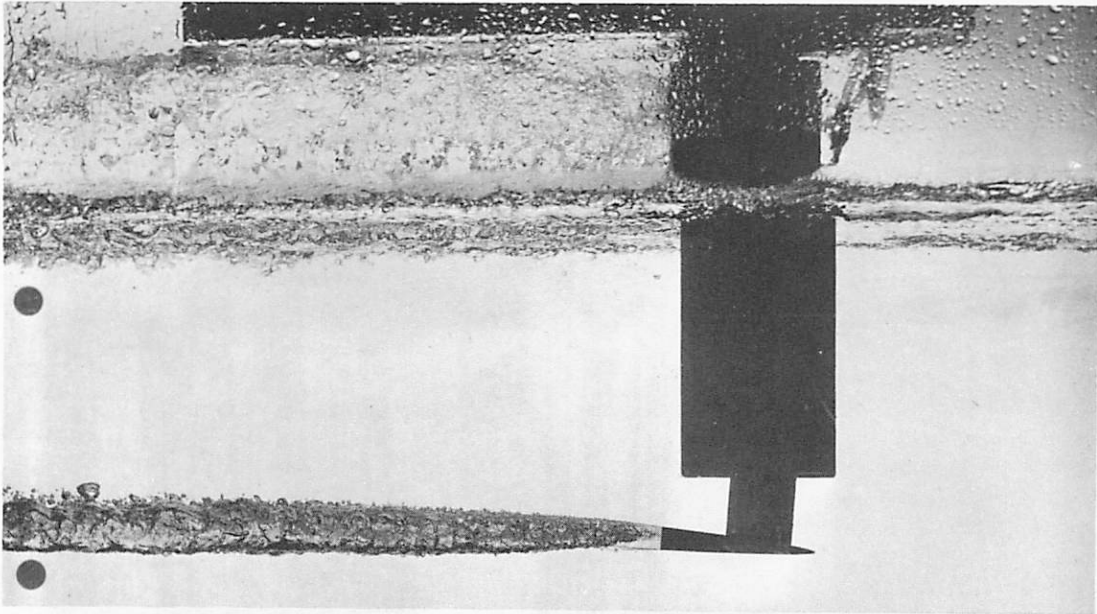


FIG. 12. Model Fully Vented, $Q' = 0.12$, $\alpha = -4.5$ deg.

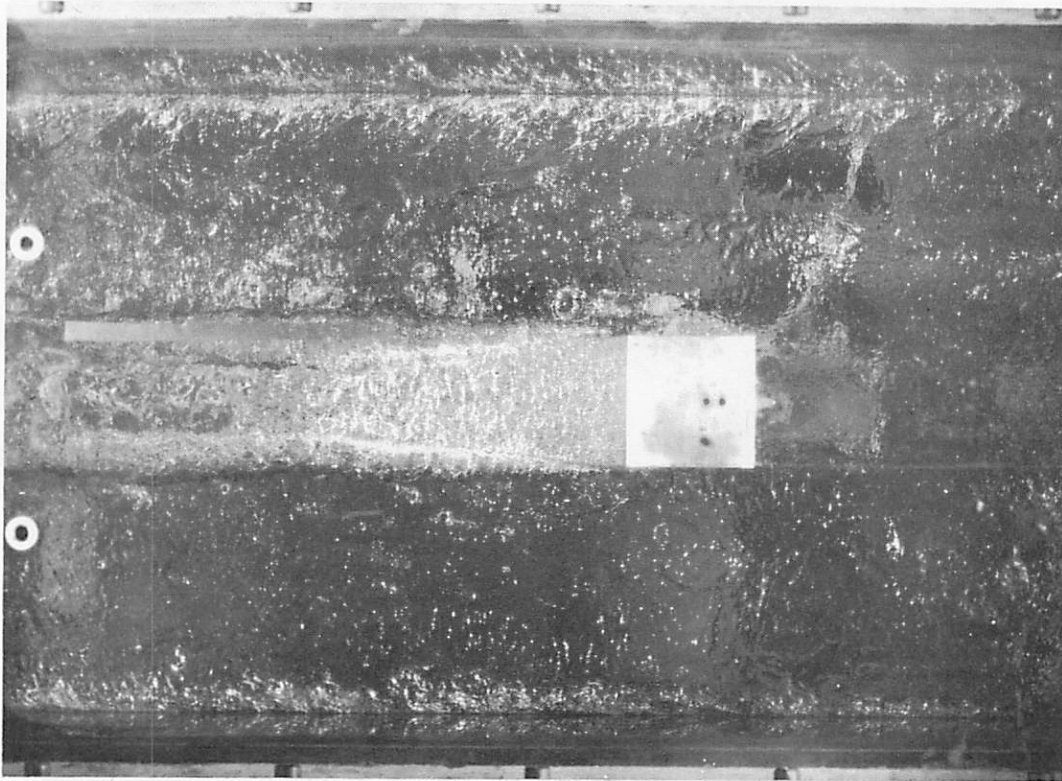


FIG. 13. Bottom View of Fully Vented Model, $Q' = 0.12$
 $\alpha = -4.5$ deg.

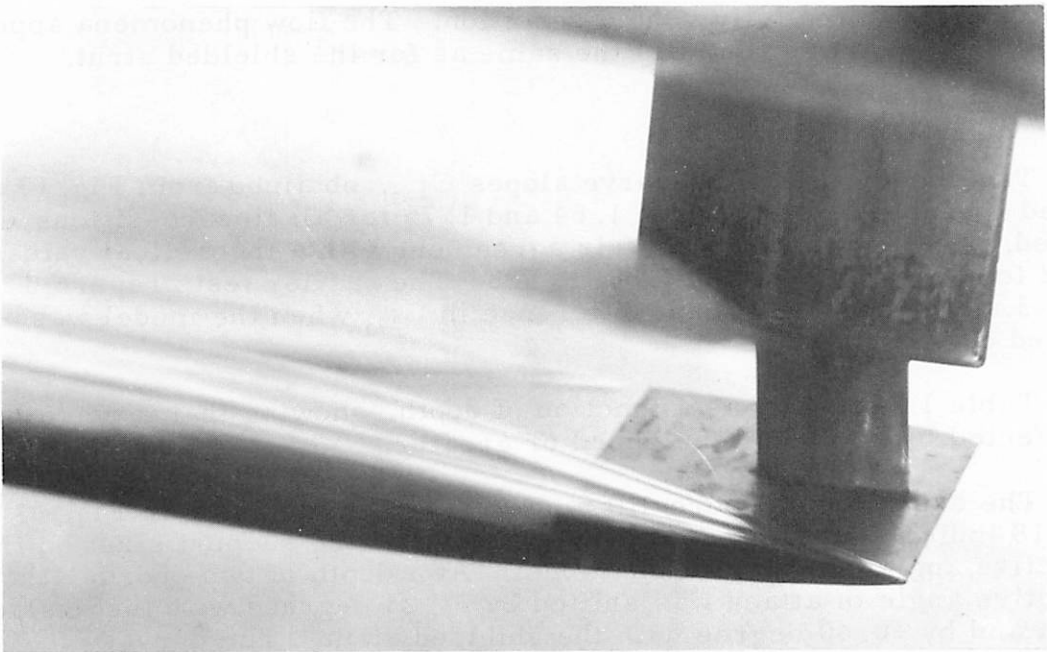


FIG. 14. Effect of Debris at Leading Edge on Cavity Shape; Model Fully Vented.

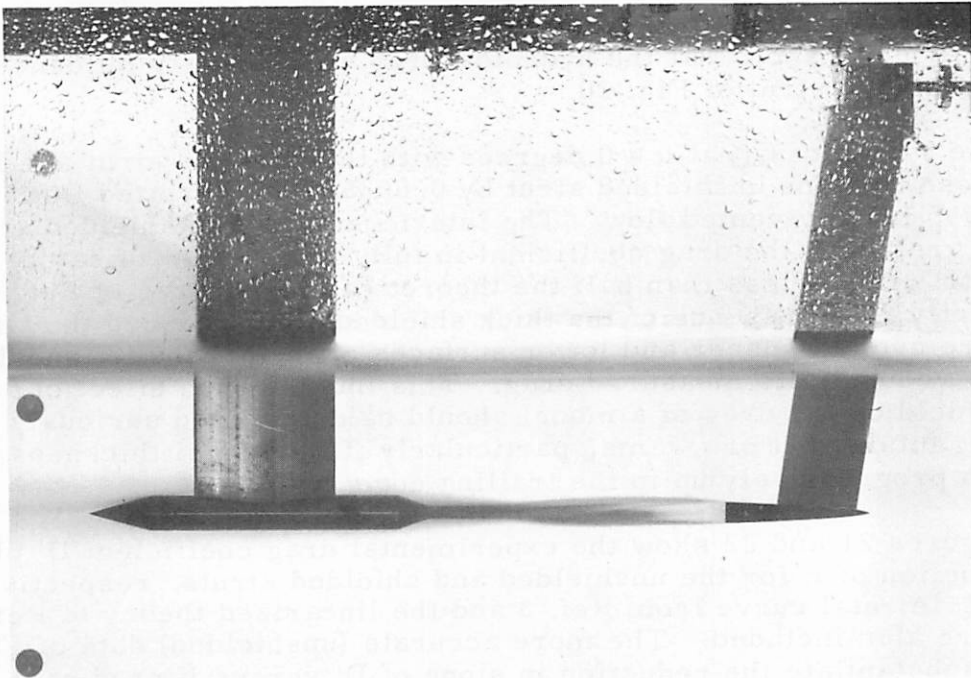


FIG. 15. Unshielded Strut and Model, Low Air-Flow Rate, $\alpha = 0$ deg.

strut pertain to the fully vented condition. The flow phenomena appearing in Fig. 16 are essentially the same as for the shielded strut.

LIFT

The experimental lift-curve slopes $C_{L\alpha}$, obtained from Fig. 17 and listed in Table 1, lie between 1.64 and 1.75 for all flow conditions tested. These values are in fair agreement with a theoretical value of 1.48 for $AR = 1.0$ obtained from Ref. 8. The earlier tests reported in Ref. 3 showed no significant difference in $C_{L\alpha}$ when the model was wetted or vented.

Table 1 lists $C_{L\alpha}$ as a function of depth, showing that it remains unaffected by depths of one chord or greater.

The experimental zero-lift angles of attack tabulated in Fig. 17 and 18 indicate a strong interference effect of the support strut on the effective angle of attack of the model. At a depth of two chords, the effective angle of attack was shifted by +1.25 degrees with the unshielded strut and by +0.40 degree with the shielded strut. The curves of Fig. 17 and 18 were shifted before plotting so that zero lift (when fully wetted) occurs at zero angle of attack, as expected for an uncambered model.

DRAG

The curves of the drag coefficient C_D versus angle of attack α (Fig. 19 and 20) show that the hydrofoil drag was strongly influenced by the shielded strut of Fig. 20.

The values of C_D at $\alpha = 0$ degrees with the shielded strut are lower than those with the unshielded strut by 0.0035 in fully wetted flow, and by 0.0095 in fully vented flow. The interference of the shielded strut was so great that the drag coefficient in fully vented flow of cavity and frictional drag is less than half the theoretical cavity drag of Ref. 4. Apparently, the presence of the thick shielded strut reduced the static pressure over the upper and lower surfaces of the parabolic model, thereby reducing its measured drag. This interference effect of a strut shield on the drag of a model should be considered seriously in planning future test programs, particularly if the model thickness increases progressively up to the trailing edge.

Figures 21 and 22 show the experimental drag coefficient D' plotted as a function of K for the unshielded and shielded struts, respectively. An experimental curve from Ref. 3 and the linearized theory of Ref. 4 and 9 are also included. The more accurate (unshielded) data of Fig. 21 do not substantiate the reduction in slope of D' versus K predicted by theory for $K < 0.10$; the disagreement may be due either to the fact that the theory is two-dimensional or that errors occurred in measuring K . It is interesting to note that the slopes of D' versus K also vary from

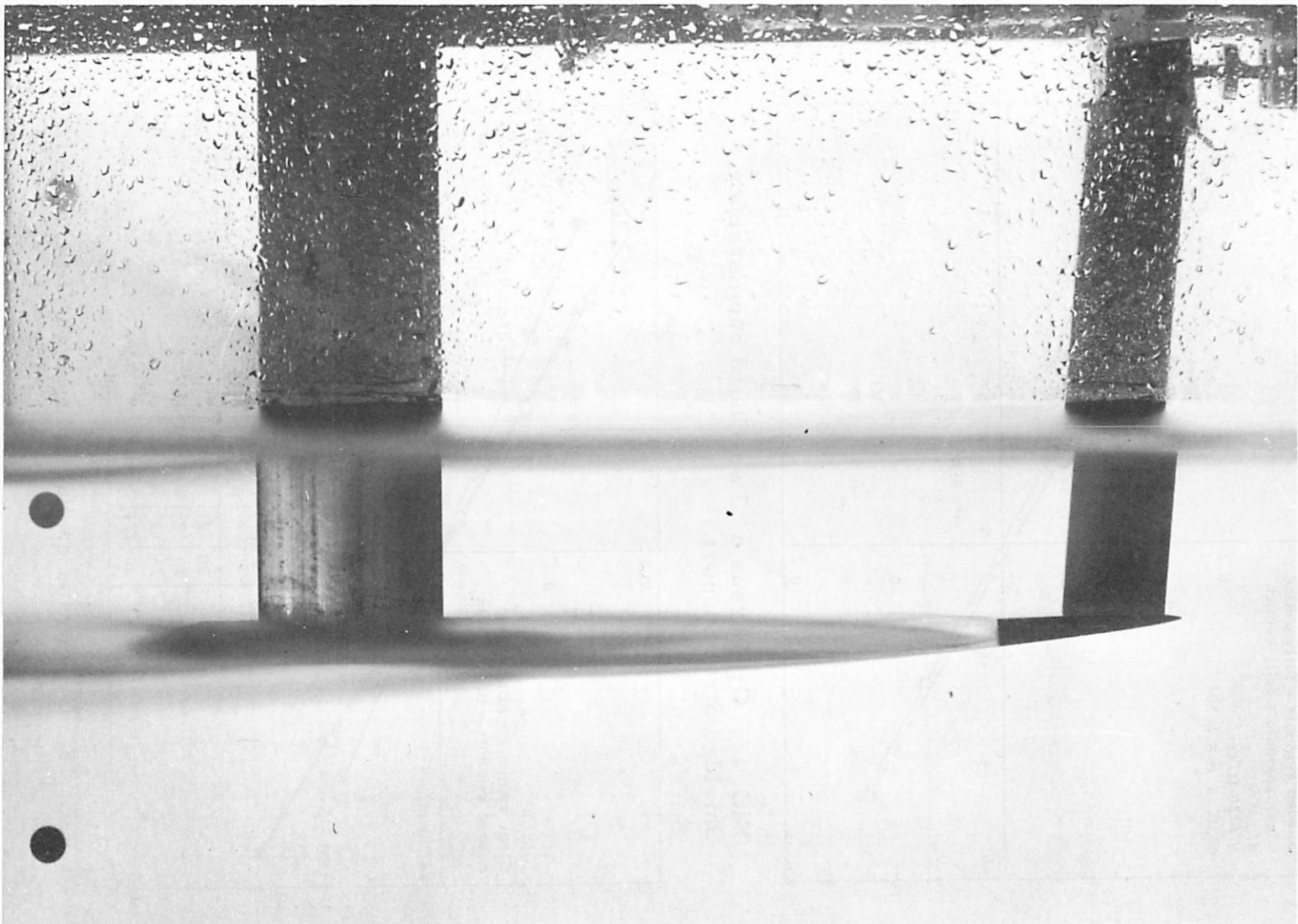


FIG. 16. Unshielded Strut and Model, $Q' = 0.09$, $\alpha = 6.6$ deg.

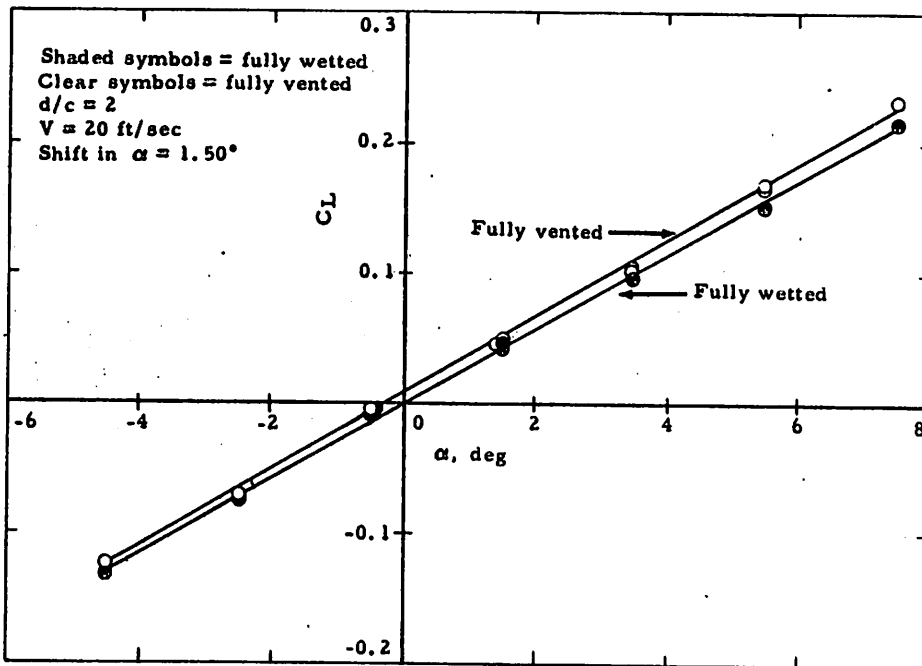


FIG. 17. C_L Versus α ; Two-Chord Submergence, Shielded Strut Support.

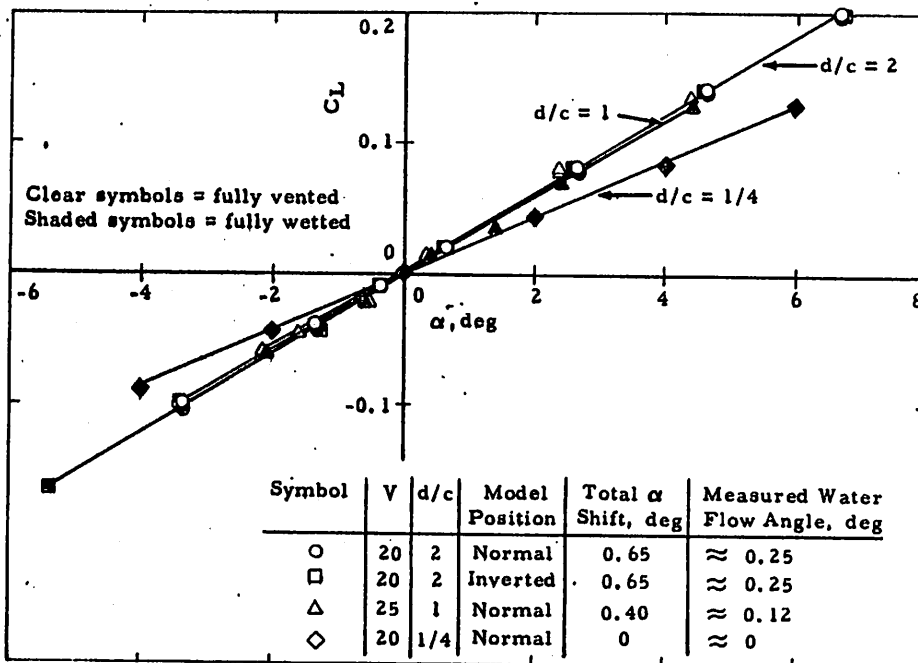


FIG. 18. C_L Versus α ; Variable Depth, Unshielded Strut Support.

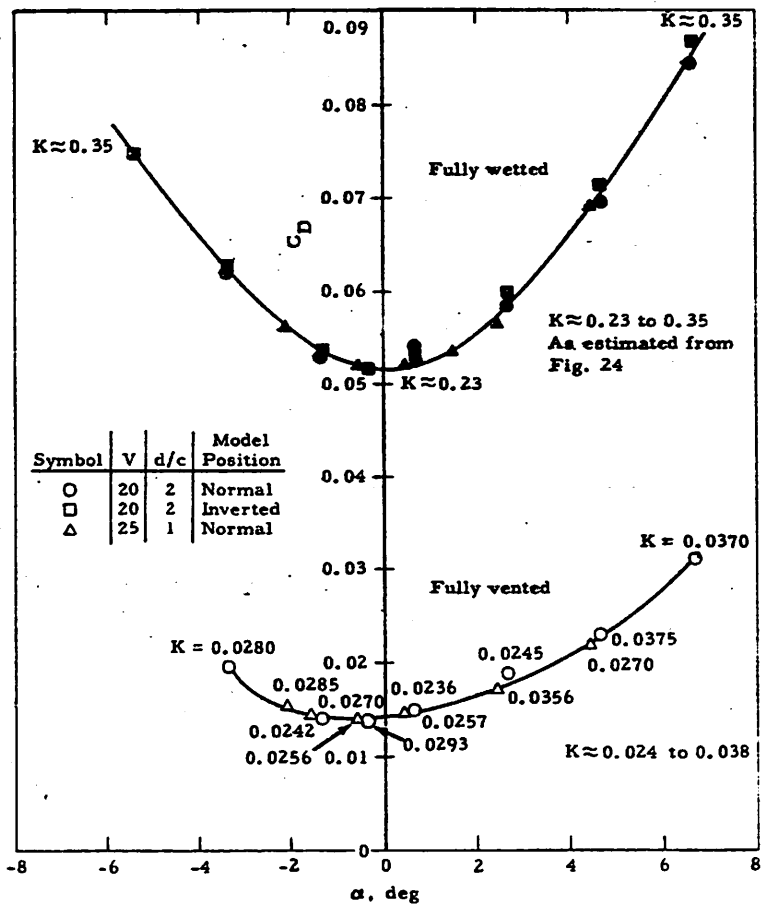


FIG. 19. C_D Versus α ; Unshielded Strut Support.

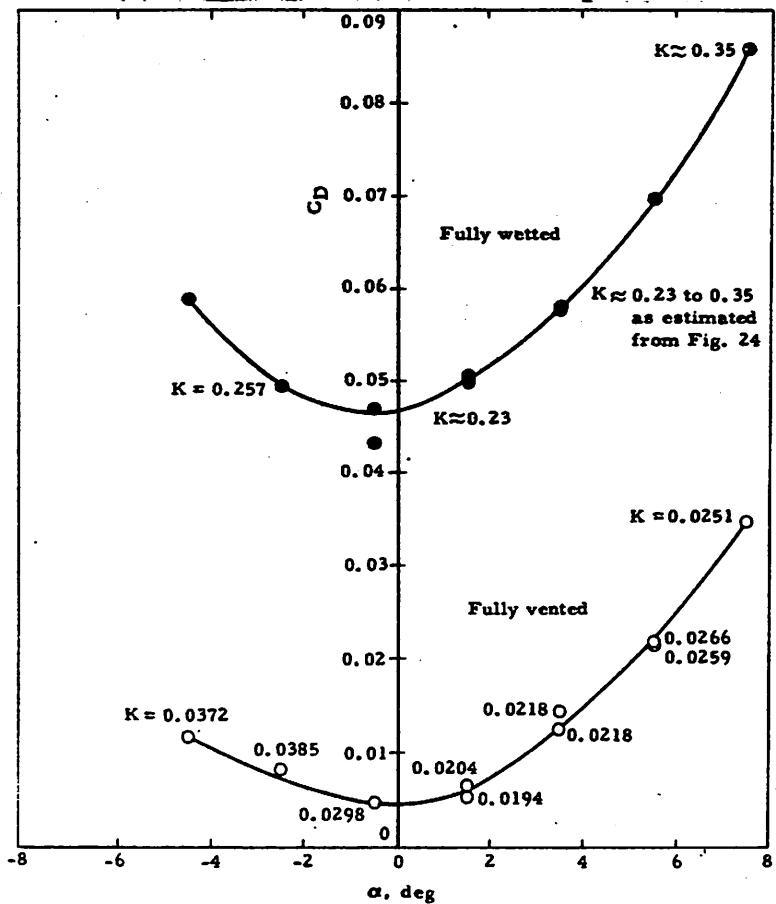


FIG. 20. C_D Versus α ; Shielded Strut Support.

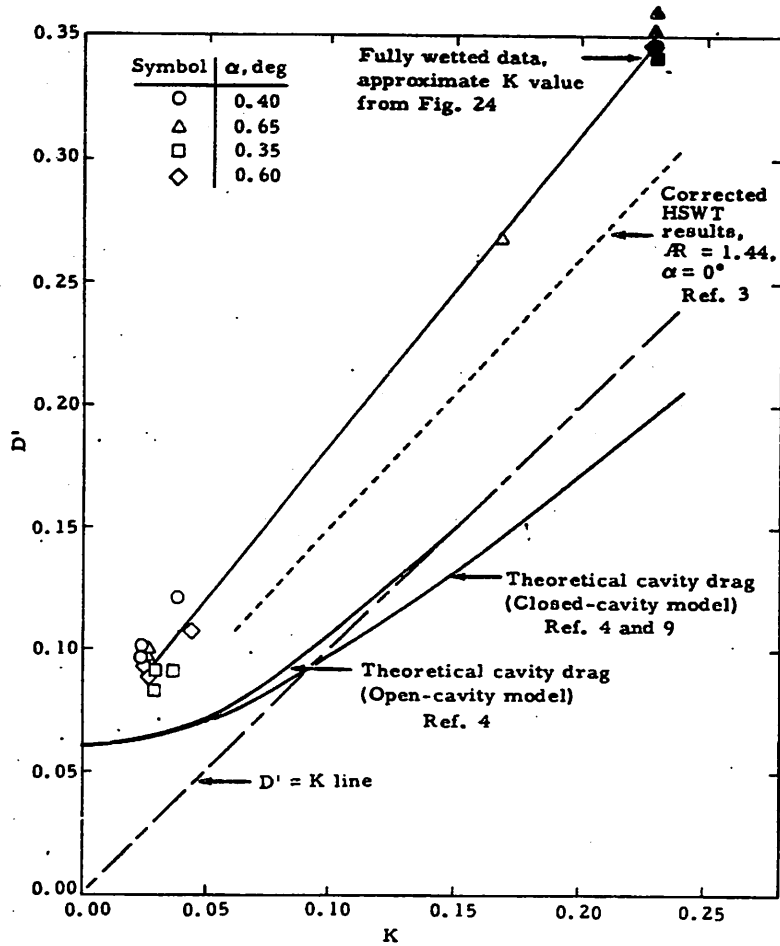


FIG. 21. Effect of Cavity Pressure on Drag; $\alpha \approx 0$ deg, Unshielded Strut Support.

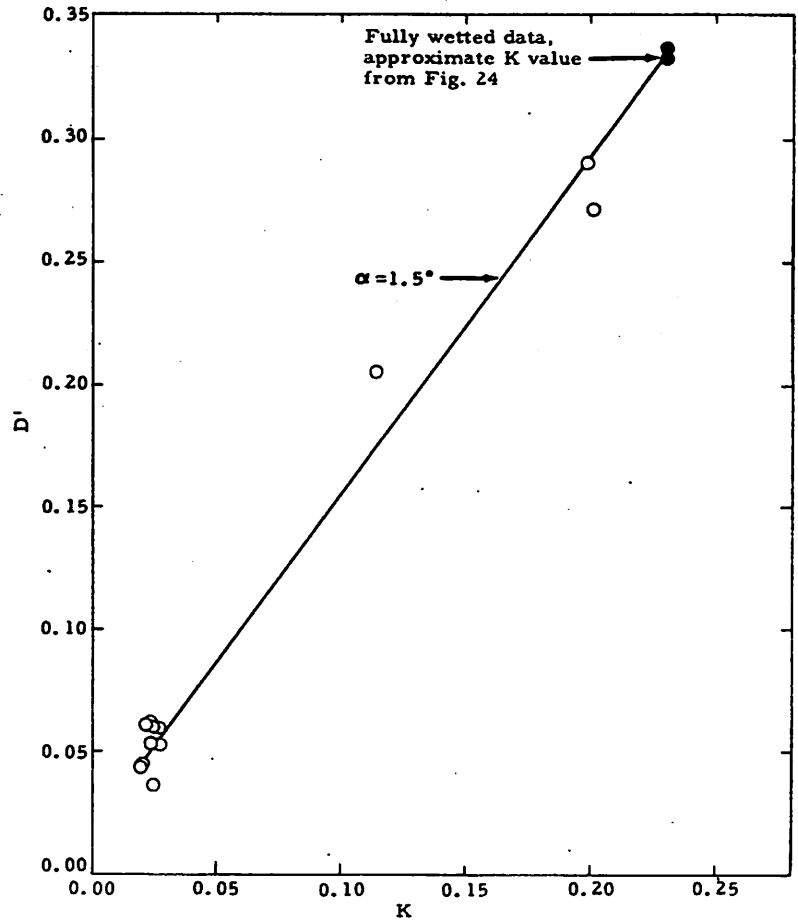


FIG. 22. Effect of Cavity Pressure on Drag; 1.5 deg, Shielded Strut Support.

the theoretical open-cavity slope of 1.00. The slopes obtained from Fig. 21 and 22 are 1.26, 1.35, and 1.08, respectively, for the current unshielded and shielded model tests and the HSWT tests of Ref. 3.

The effect of α on model drag can be studied by analyzing the unshielded strut data of Fig. 19. The shielded strut data are not used in this analysis because of the potentially large strut interference. In general, the variation of C_D with α for low-aspect-ratio hydrofoils is most likely due not only to the induced drag but also to changes with α of separation drag, cavity drag, and frictional drag. Theoretically, the induced drag is approximately equal to $C_L^2/\pi AR$. When analyzing the variation of C_D with α , it is convenient to study the drag factor, $\pi AR C_D^2/C_L^2$. The difference between the experimental drag factor and the theoretical induced drag factor of 1.0 represents the approximate contributions of separation drag, cavity drag, and frictional drag. The total experimental drag factor was 1.37 for fully vented flow, and 2.86 for fully wetted flow.

In considering the cavity drag first, Fig. 19 shows that the ventilation number K remained constant and independent of α when the model was fully vented. When the model was fully wetted, K varied from 0.23 to 0.35. Combining the experimental variation of drag with K (Fig. 21) and the variation of K with α , the contribution of cavity drag to the drag factor can be calculated. This contribution is about 1.77 for the unshielded strut in fully wetted flow. The contribution is zero in fully vented flow. The remaining portion of the drag factor is 0.09 in fully wetted flow and 0.37 in fully vented flow. This portion is probably caused by changes in separation and frictional drag resulting from changes in pressure distribution and boundary layer state. The pressure distribution changes differently in fully wetted and fully vented flow because the cavity pressure changes differently with α . The drag factor for the model is divided as follows:

<u>Drag Factor</u>	<u>Fully Wetted</u>	<u>Fully Vented</u>
Total	2.86	1.37
Induced	1.00	1.00
Cavity	1.77	0.00
Separation and skin friction . . .	0.09	0.37

MOMENT COEFFICIENT

The only moment data taken were on the model supported by the shielded strut. Although many of these data were undoubtedly affected by strut interference, it is believed that the effect of K on C_M remained relatively small. The data plotted in Fig. 23 show considerable scatter but indicate that C_M was essentially independent of the ventilation number K , as might be expected from theory.

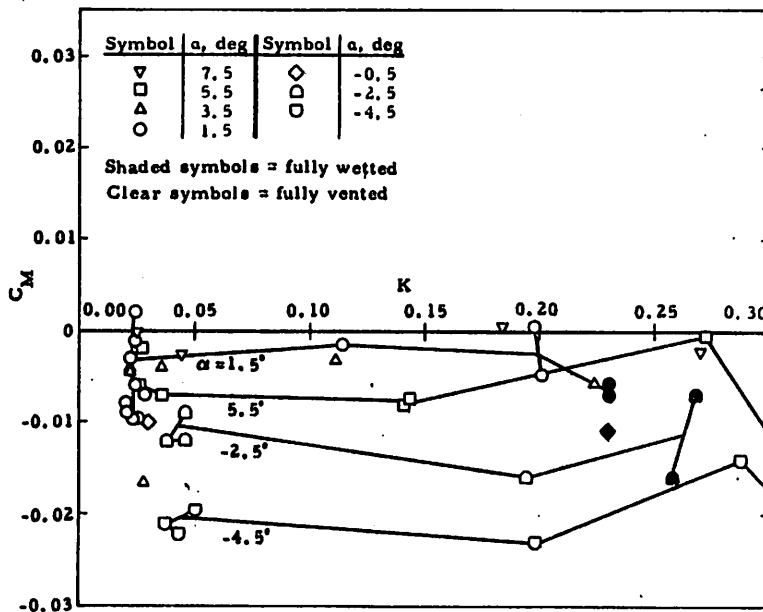


FIG. 23. C_M Versus α and K ; Shielded Strut Support.

The moment coefficient at $\alpha = 0$ degrees varied between -0.010 to $+0.002$. Since the model was uncambered, this value should be zero. The center of pressure can be calculated from the variation of C_M and C_L with α . The experimental results show that the center of pressure lies at the 20 to 29% chord point when fully wetted. The difference between these and the theoretical value of 17% is explained by the inaccuracy of the C_M data and strut interference.

AIR-FLOW RATE

The curves of K versus Q' and α are plotted in Fig. 24. In Fig. 25 results of earlier tests conducted in the HSWT are reproduced from Ref. 3 for comparison.

The most significant difference in results between the two tunnels is the change in the critical air-flow rate coefficient, Q'_{cr} . This coefficient represents the minimum air-flow rate required to first fully ventilate the hydrofoil. The difference in blockage between the two water tunnels seems to be responsible for the reduction in Q'_{cr} from 0.07 in the enclosed HSWT to 0.026 in the FSWT. This indicates that much less gas is required to ventilate prototype configurations than was previously believed. The effect of hysteresis is the same in both tunnels in the sense that the air-flow rate could be reduced to about half the value of Q'_{cr} before the fully vented cavity shape changed back into the partially vented vortex-type cavity shape.

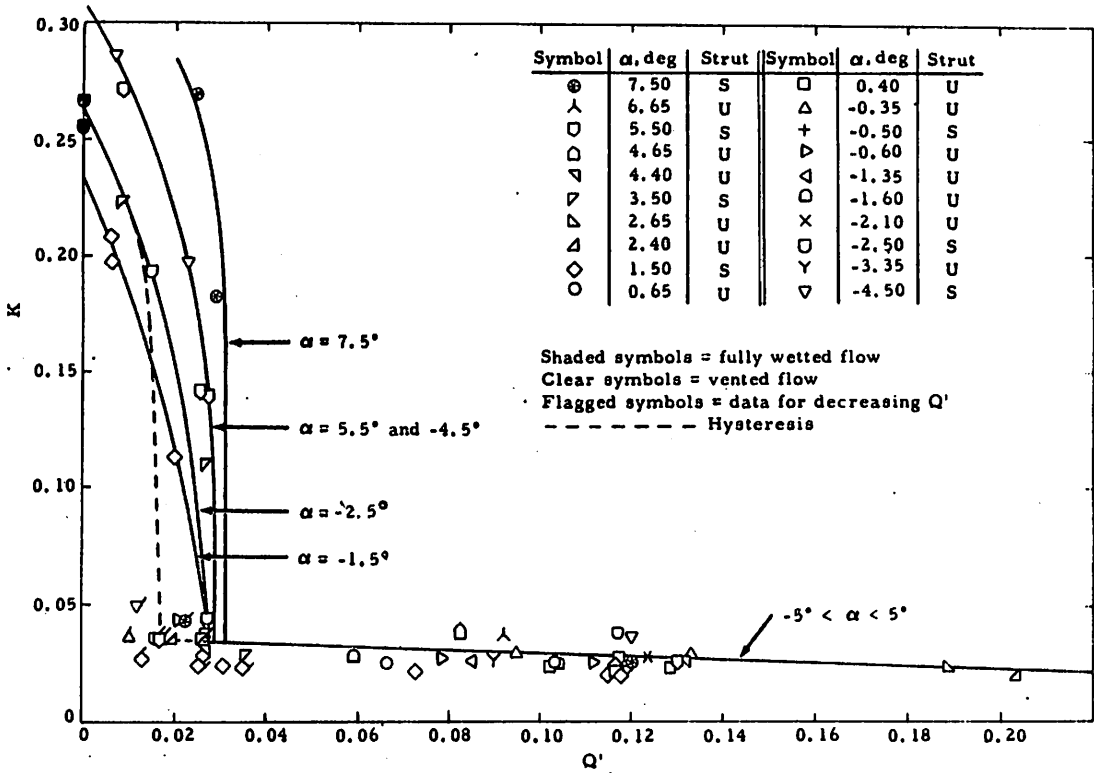


FIG. 24. Effect of Air-Flow Rate and Angle of Attack on Ventilation Number; Both Strut Supports.

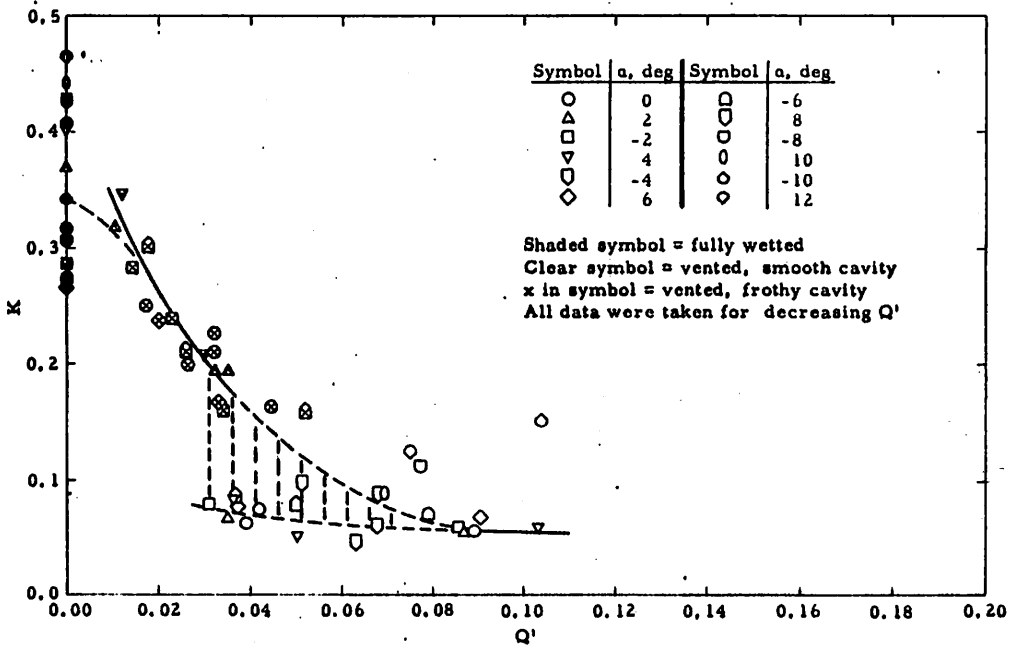


FIG. 25. K Versus Q' With $AR = 1.44$. Data from high speed water-tunnel experiments (Ref. 3).

The data in Fig. 24 show that the results of the shielded and unshielded struts were essentially the same. No data could be taken in the partially vented range with the unshielded strut because of the air-exhaust method used.

VENTILATION NUMBER

It is desirable in practice to obtain as low a ventilation number as possible, since the drag reduces as K reduces. The test results in Ref. 3 showed that K could not be reduced below 0.15 in the two-dimensional tunnel section, or below 0.06 in the three-dimensional tunnel section of the HSWT. One of the reasons for conducting the current tests was to obtain new data on minimum K in a tunnel that is essentially unaffected by wall interference and therefore more representative of open-water prototype operation.

The minimum value of K measured in the current series was 0.02. No interference by the strut shield was noticed. Once the hydrofoil was fully vented, the value of K reduced only slightly with large increases in air-flow rate. It would not be worth while from a power or efficiency viewpoint to attempt to reduce K below 0.02 by increasing the air-flow rate. It is probable that the minimum value of K obtained in the FSWT is representative of the minimum obtainable in open-water operation.

The ventilation number is shown in Fig. 26 to have no effect on lift coefficient. Essentially the same result was observed in Ref. 3, except for a small deviation in the range where $K < 0.20$. This small deviation (Ref. 3) was believed to be due to the model camber, which caused the flow to separate from the upper surface near its trailing edge when $K < 0.20$.

LIFT-TO-DRAG RATIO

The maximum lift-to-drag ratio L/D (Fig. 27) is 2.4 when fully wetted and 6.5 when fully vented (model $AR = 1.0$ and unshielded strut). These values compare favorably with the corresponding values of 4.0 and 8.5 (Ref. 3) for a cambered model with $AR = 1.44$ tested in the HSWT. These results demonstrate the advantages of increased aspect ratio, of camber, and of reduced ventilation number. Even higher values of L/D could be obtained if the ventilation number K were reduced to zero.

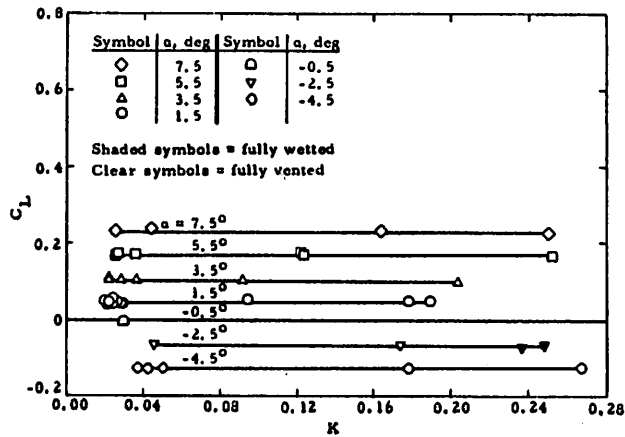


FIG. 26. Effect of Ventilation Number on C_L ; Shielded Strut Support.

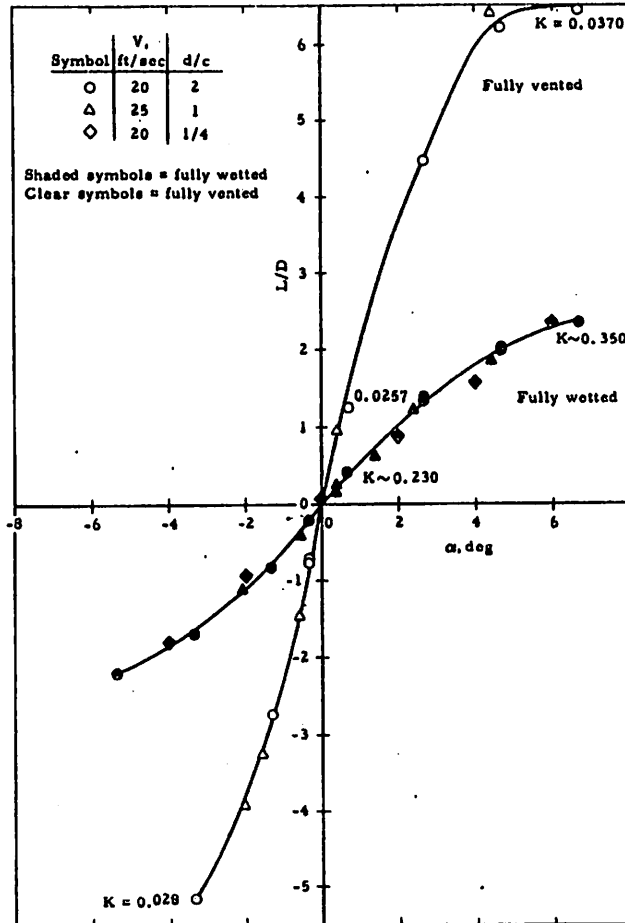


FIG. 27. Lift-to-Drag Ratios Versus α ; Unshielded Strut Support.

CONCLUSIONS

The following conclusions are drawn from this study.

1. The minimum air-flow rate coefficient Q'_{cr} required to first form a fully vented cavity behind the blunt trailing edge of the model was 0.026 (air-flow rate increasing); hysteresis occurred since Q'_{cr} was 0.013 (air-flow rate decreasing). Considerable tunnel-wall blockage must have occurred in the earlier test work (Ref. 3) that was conducted in the enclosed HSWT at CIT, since the values of Q'_{cr} were 0.07 and 0.03, respectively.
2. Once the cavity was fully vented, the cavity pressure could not be significantly changed, even with a large increase in air-flow rate.
3. The air cavity produced behind the base of the model did not spring ahead of the base at any angle of attack throughout the test range of +7.5 degrees down to -4.5 degrees, except when debris stuck to the leading edge.
4. Because of reduced tunnel blockage in the FSWT, the minimum ventilation number K_{min} was found to be 0.02. This value is probably more representative of open-water prototype conditions than the value of $K_{min} = 0.06$ (Ref. 3) for the HSWT.
5. The maximum lift-to-drag ratio L/D was 2.4 when fully wetted and 6.5 when fully vented. These values are typical for uncambered hydrofoils of $AR = 1$. Higher values of L/D would result if the aspect ratio were increased and camber were used (Ref. 3).
6. The values of C_L , $C_{L\alpha}$, and C_M were essentially independent of K and did not vary appreciably whether the model was fully wetted or fully vented. This result agrees with the theory of Ref. 5, page 14.
7. The value of $C_{L\alpha}$ was independent of depth for depths greater than one chord.
8. The drag coefficient only partially agreed with two-dimensional cavity theory. No change in slope was observed in the experimental graph of D' versus K as K approached zero, as predicted by theory. Also, the slope of D'/K at higher values of K was 25 to 35% greater than the theoretical value of 1.0.
9. Considerably more increase in drag with angle of attack α was noticed when the model was fully wetted than when it was fully vented. This was due to a greater increase in cavity (or wake) drag produced by a large change in K with α when the model was fully wetted. There was essentially no change of K with α when the model was fully vented.
10. From a test-method viewpoint it was found that much less interference occurred when the model was supported by an unshielded strut than when it was supported by a shielded strut. In the latter case, the interference can be so large that the model drag, for example, can be changed by a factor of two or three.

Appendix A

CORRECTIONS APPLIED TO THE FORCE DATA

STRUT TARE FORCES

The shielded strut tare forces were measured with the model mounted at a depth of two chords on an image strut projecting upward from the tunnel floor. The shielded strut was then lowered until there was a very small gap between it and the model. The forces were measured at three angles of attack (0° , $+6^\circ$, and -6°), in fully wetted flow only. The strut tare drag, moment, and lift coefficients, based on planform area, are shown in Fig. 28. The tare drag and moment coefficients appear reasonable, but the lift coefficient is slightly negative. It is possible that the negative lift was caused by reduced pressure in the gap between the strut and the model. Since this correction was small and possibly meaningless, it was not applied.

The unshielded strut tare forces were measured without the model. The model was removed from the strut and the lower end of the strut was faired to a streamlined shape with wax. Runs were made at the angle of attack where the lower end of the strut was horizontal. Data were taken at velocities of 20 and 25 ft/sec and at several submergence values. The drag coefficient of the strut, based on the model planform area, is plotted in Fig. 29 versus submergence. The lift coefficient of the strut was rather scattered. The correction to the model lift coefficient was obtained by adding the calculated buoyancy of the model, in coefficient form, to the measured strut lift coefficients and fairing a curve through the resulting points. The correction curves for velocities of 20 and 25 ft/sec are shown in Fig. 30. Also shown are lift measurements made at zero velocity for various model depths, which are about equal to the buoyancy of the model and strut, but do not include the hydrodynamic lift of the strut. It is noted that a fixed amount of buoyancy produces a lift coefficient that depends upon the reference velocity.

Another correction applied to the unshielded strut data is due to the thrust of the air jet on the model. This correction is plotted in Fig. 31. The coefficient is based upon a reference velocity of 20 ft/sec.

A final correction to the force coefficients is needed since the tunnel-flow direction was not parallel to the drag axis. The true lift and drag forces should be normal to, and parallel to, the stream direction (Fig. 32). The relation between the measured and true forces was

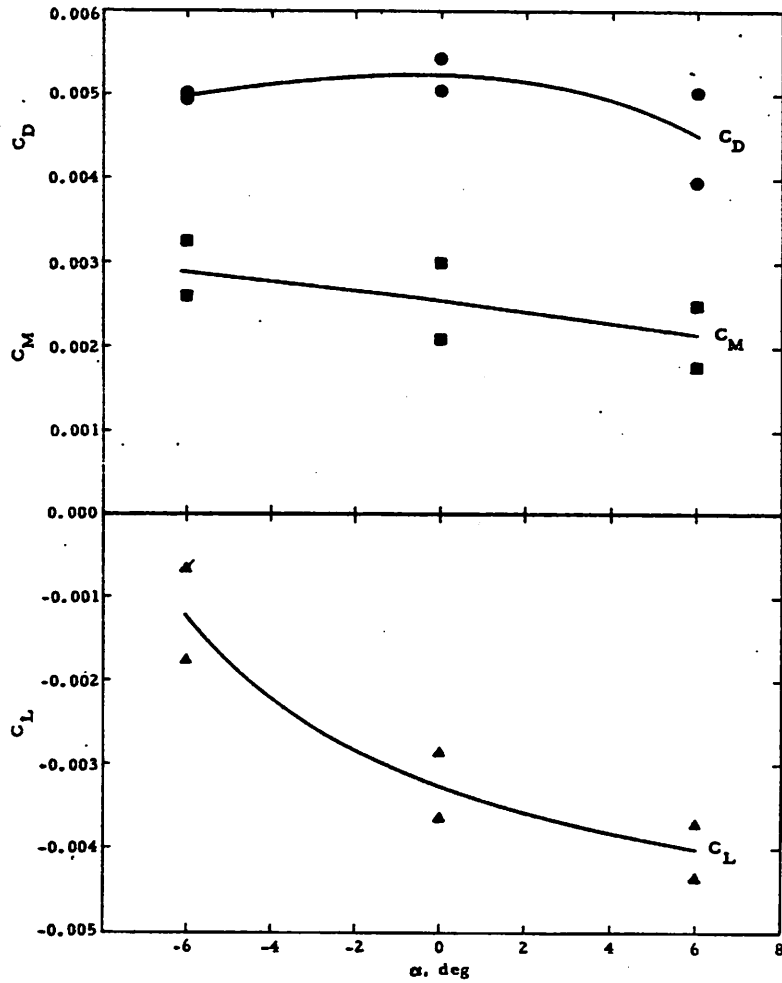


FIG. 28. Tare Corrections for Model Strut in Shielded Strut Support System.

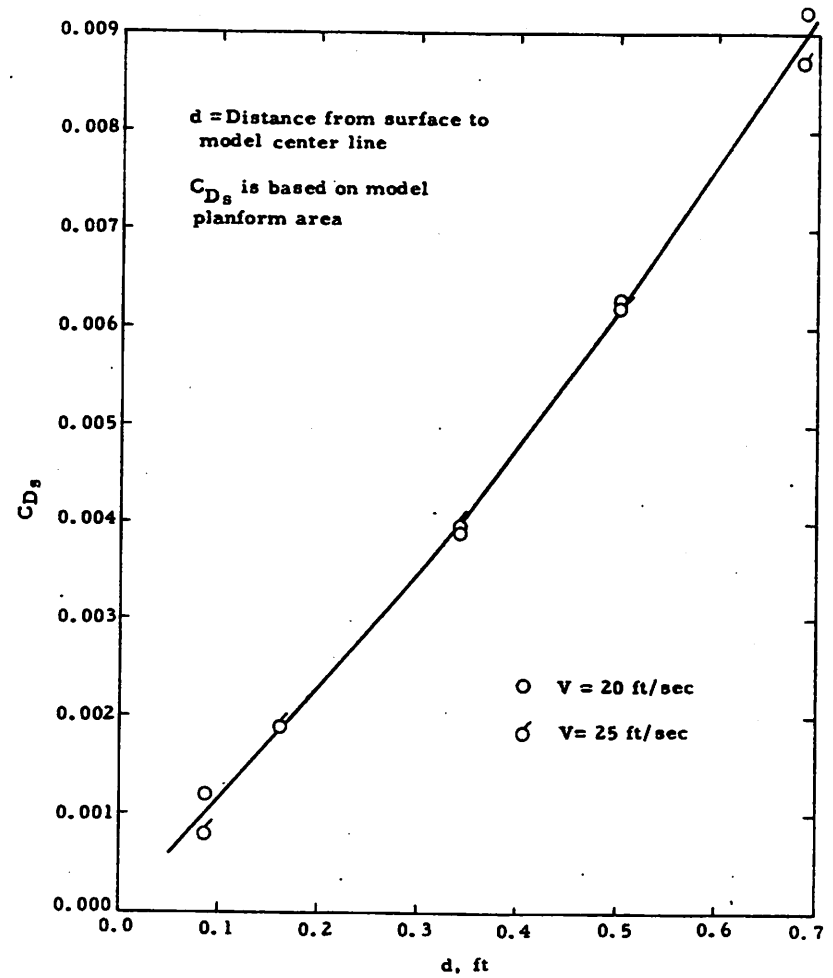


FIG. 29. Tare Correction for Frictional Drag of Unshielded Strut Versus Model Depth.

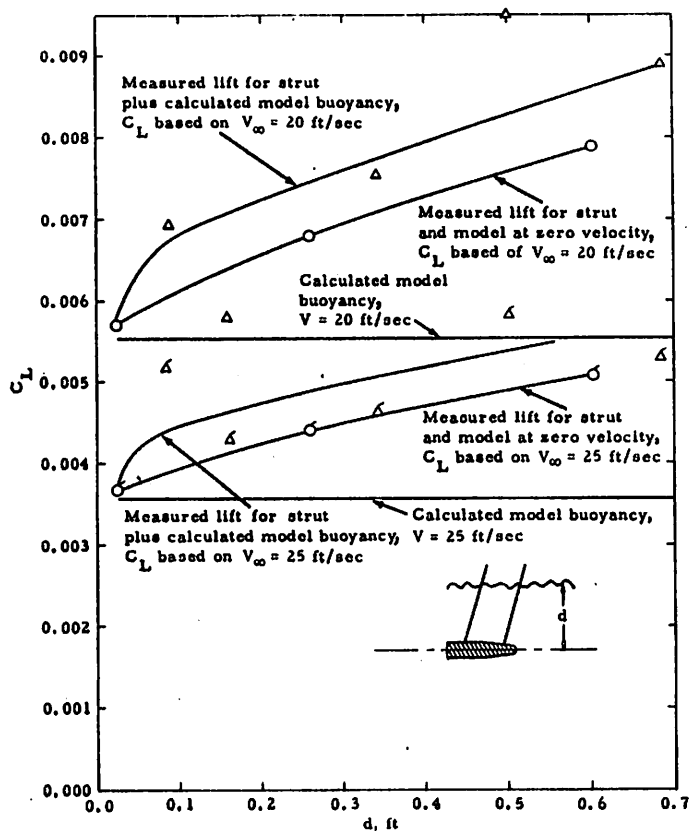


FIG. 30. Tare Correction for Lift of Unshielded Strut Versus Model Depth.

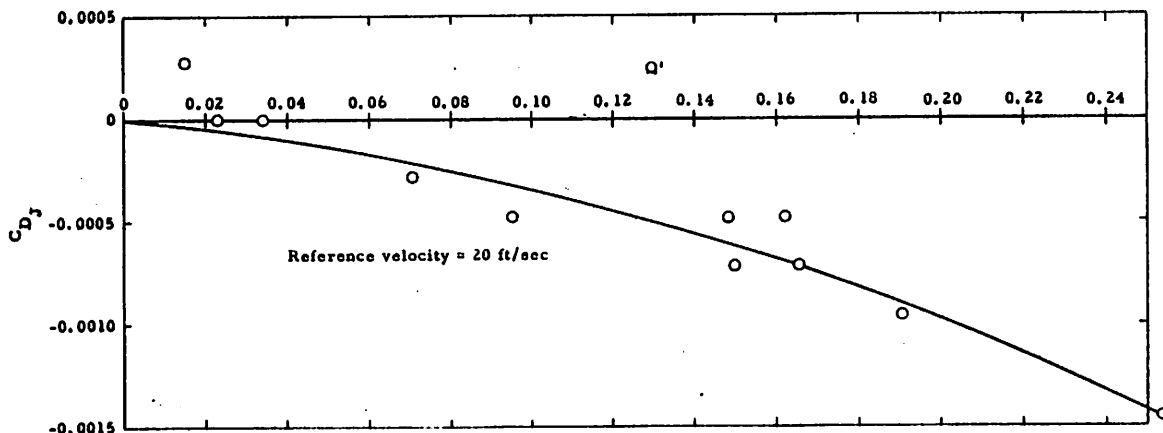


FIG. 31. Tare Correction for Air-Jet Thrust on Model; Unshielded Strut Support.

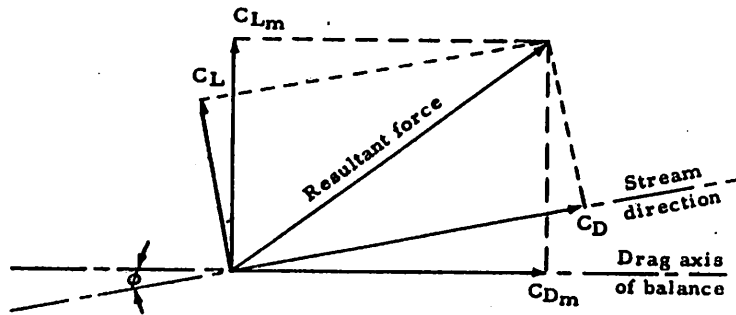


FIG. 32. Correction of Data Due to Nonaxial Tunnel Water Flow.

calculated by assuming that $\phi = -\alpha_0$ (where α_0 is the value of the experimental α at which $C_L = 0$, after being corrected for tare and buoyancy).

$$C_L = C_{L_{meas}} \cos \alpha_0 + C_{D_{meas}} \sin \alpha_0$$

$$C_D = C_{D_{meas}} \cos \alpha_0 - C_{L_{meas}} \sin \alpha_0$$

The correction to C_L was negligible, but the correction to C_D was significant at higher angles of attack.

Appendix B

AIR-FLOW DATA REDUCTION

The air flowmeter is calibrated to measure the air-flow rate at standard room temperature and standard pressure P_s . Since the air passing through the meter is at the supply-line pressure P_l , the meter reading Q_m must be corrected. Since the supply-line air is at room temperature, its density will be proportional to its pressure P_l , hence:

$$Q_m = Q_l \sqrt{\frac{P_l}{P_s}} \quad \text{or} \quad Q_l = Q_m \sqrt{\frac{P_s}{P_l}}$$

The air-flow rate Q based on the freestream static pressure P_∞ is $Q = Q_l (P_l/P_\infty)$. It is assumed that the air lines from the flowmeter to the working section are long enough to cause the flow to become isothermal. Hence, the air-flow rate at a pressure P_∞ is

$$Q = Q_l \frac{P_l}{P_\infty} = Q_m \frac{P_l}{P_\infty} \sqrt{\frac{P_s}{P_l}}$$

The dimensionless air-flow-rate coefficient is defined as:

$$Q' = \frac{Q}{V_\infty A_b}$$

The actual pressure in the cavity is slightly different from the freestream static pressure, but since the difference is small the actual air-flow rate is approximately equal to Q .

REFERENCES

1. U. S. Naval Ordnance Test Station. Base-Vented Hydrofoils, by T. G. Lang. China Lake, Calif., NOTS, 19 October 1959. (NAVORD Report 6606, NOTS TP 2346.)
2. ----- . Water-Tunnel Tests of Hydrofoils With Forced Ventilation, by Thomas G. Lang, Dorothy A. Daybell, and Kenneth E. Smith. China Lake, Calif., NOTS, 10 November 1959. (NAVORD Report 7008, NOTS TP 2363.)
3. ----- . Water-Tunnel Tests of a Base-Vented Hydrofoil Having a Cambered Parabolic Cross Section, by Thomas G. Lang and Dorothy A. Daybell. China Lake, Calif., NOTS, 10 October 1960. (NAWWEPS Report 7584, NOTS TP 2569.)
4. ----- . Application of Thin-Airfoil Theory to Hydrofoils With Cut-Off, Ventilated Trailing Edge, by Andrew G. Fabula. China Lake, Calif., NOTS, 13 September 1960. (NAWWEPS Report 7571, NOTS TP 2547.)
5. ----- . Linearized Theory of Vented Hydrofoils, by A. G. Fabula. China Lake, Calif., NOTS, 7 March 1961. (NAWWEPS Report 7637, NOTS TP 2650.)
6. Knapp, T. T., J. Levy, J. P. O'Neill, F. B. Brown. "The Hydrodynamics Laboratory of the California Institute of Technology," AM SOC MECH ENG, TRANS, Vol. 70, No. 5 (July 1948), pp. 437 - 57.
7. California Institute of Technology. An Experimental Study of the Hydrodynamic Forces Acting on a Family of Cavity Producing Conical Bodies of Revolution Inclined to the Flow, by Taras Kiceniuk. Pasadena, Calif., CIT, June 1954. (CIT Hydrodynamics Laboratory Report E-12. 17.)
8. National Advisory Committee for Aeronautics. Summary of Airfoil Data, by I. H. Abbott, A. E. von Doenhoff, and L. S. Stivers. Washington, NACA, 1945. (NACA Report No. 824.)
9. California Institute of Technology. A Simple Method for Calculating the Drag in the Linear Theory of Cavity Flows, by T. Yao-tsu Wu. Pasadena, Calif., CIT, August 1957. (CIT Engineering Division Report No. 85-5.)

ACKNOWLEDGMENT

The authors wish to acknowledge the assistance of Dr. A. Acosta, Dr. T. Wu, Dr. V. Vanoni, Dr. A. Ellis, and particularly Taras Kiceniuk of the California Institute of Technology for contributing many valuable suggestions to this study. The help of Harry Hamagouchi in obtaining force measurements, Carl Eastvedt for photographs, and Jake Brentjes for performing some of the strut interference studies is also appreciated. The aid of Glenn Bowlus of NOTS is also acknowledged for designing the shielded strut and making model drawings.

INITIAL DISTRIBUTION

- 10 Chief, Bureau of Naval Weapons
 - DLI-31 (2)
 - R-12 (1)
 - RAAD-3 (1)
 - RRRE (1)
 - RRRE-4 (1)
 - RU (1)
 - RUTO (1)
 - RUTO-32 (2)
- 6 Chief, Bureau of Ships
 - Code 106 (1)
 - Code 335 (1)
 - Code 421 (2)
 - Code 442 (1)
 - Code 664 (1)
- 1 Chief of Naval Operations
- 3 Chief of Naval Research
 - Code 429 (1)
 - Code 438 (1)
 - Code 466 (1)
- 5 David W. Taylor Model Basin
 - Code 142 (1)
 - Code 500 (1)
 - Code 513 (1)
 - Code 526 (1)
 - Code 580 (1)
- 1 Naval Academy, Annapolis (Librarian)
- 1 Naval Air Development Center, Johnsville
- 1 Naval Aircraft Torpedo Unit, Quonset Point
- 1 Naval Civil Engineering Laboratory, Port Hueneme (Code L54)
- 1 Naval Engineering Experiment Station, Annapolis
- 1 Naval Ordnance Laboratory, White Oak (Library Division, Desk HL)
- 1 Naval Postgraduate School, Monterey (Library, Technical Reports Section)
- 1 Naval Research Laboratory
- 1 Naval Torpedo Station, Keyport (Quality Evaluation Laboratory, Technical Library)
- 1 Naval Underwater Ordnance Station, Newport
- 1 Naval War College, Newport (Institute of Naval Studies)
- 1 Naval Weapons Laboratory, Dahlgren
- 2 Naval Weapons Services Office
- 1 Navy Electronics Laboratory, San Diego

- 1 Navy Mine Defense Laboratory, Panama City
- 1 Navy Underwater Sound Laboratory, Fort Trumbull
- 1 Office of Naval Research Branch Office, Pasadena
- 1 Army Research Office, Durham
- 1 Air Force Office of Scientific Research (Mechanics Division)
- 10 Armed Services Technical Information Agency (TIPCR)
- 1 Director of Defense (R&E) (Office of Fuels, Materials and Ordnance, Byard Belyea)
- 1 Committee on Undersea Warfare
- 1 Maritime Administration (Coordinator for Research)
- 1 Merchant Marine Academy, Kings Point, N. Y. (Head, Department of Engineering)
- 6 National Aeronautics and Space Administration
- 1 National Bureau of Standards (Fluid Mechanics Section, Dr. G. Schubauer)
- 2 National Science Foundation
 - Director (1)
 - Director, Engineering Sciences Division (1)
- 5 British Joint Services Mission (Navy Staff), via BuWeps (DSC)
- 2 Defence Research Member, Canadian Joint Staff (W), via BuWeps (DSC)
- 2 Aerojet-General Corporation, Azusa, Calif., via BuWepsRep
 - J. Levy (1)
 - Library (1)
- 1 Aeronutronic, Newport Beach, Calif. (Library)
- 1 Airesearch Manufacturing Company, Los Angeles (Dr. B. R. Parkin)
- 1 Alden Hydraulic Laboratory, Worcester Polytechnic Institute, Worcester, Mass.
- 1 American Mathematical Society, Providence, R. I. (Editor, Mathematical Review)
- 1 Applied Physics Laboratory, University of Washington, Seattle
- 1 AVCO Research Laboratory, Everett, Mass. (Technical Library)
- 1 Baker Manufacturing Company, Evansville, Wisc.
- 1 Bell Aerosystems Company, Buffalo (Technical Library)
- 1 Brown University, Providence, R. I. (Division of Engineering)
- 1 Bulova Research and Development Laboratories, Inc., Woodside, N. Y.
- 3 California Institute of Technology, Pasadena (Engineering Division)
 - Dr. C. B. Millikan (1)
 - Dr. M. S. Plesset (1)
 - Dr. V. A. Vanoni (1)
- 1 Case Institute of Technology, Cleveland (Department of Mechanical Engineering)
- 1 Clevite Ordnance, Cleveland (Library)
- 1 Colorado State University, Fort Collins (Department of Civil Engineering)
- 1 Convair, San Diego (Engineering Library)
- 1 Convair Hydrodynamics Laboratory, San Diego
- 1 Convair Scientific Research Laboratory, San Diego
- 1 Cornell Aeronautical Laboratory, Inc., Buffalo (Department 410)

- ① Cornell University, Graduate School of Aeronautical Engineering,
Ithaca (Library)
- 2 Davidson Laboratory, Stevens Institute of Technology, Hoboken, N. J.
A. Suarez (1)
Dr. J. Breslin (1)
- 1 Douglas Aircraft Company, Inc., Long Beach (Aerodynamics Section)
- 1 Eastern Research Group, New York City
- 1 EDO Corporation, College Point, N. Y. (Library)
- 1 Electric Boat Division, General Dynamics Corporation, Groton, Conn.
(Library)
- ① Engineering Societies Library, New York City
- 1 General Electric Company, Defense Electronics Division, Pittsfield,
Mass. (Engineering Librarian)
- 1 General Electric Company, Schenectady (Librarian, LMEE Department)
- ② Gibbs and Cox, Inc., New York City
Dr. S. Hoerner (1)
Library (1)
- ① Grumman Aircraft Engineering Corporation, Bethpage, N. Y. (Library)
- 1 Harvard University, Cambridge, Mass. (Department of Engineering
Sciences)
- 1 Hughes Aircraft Company, Culver City, Calif. (Library)
- ⑤ Hydrodynamics Laboratory, CIT, Pasadena
Dr. A. J. Acosta (1)
Dr. A. T. Ellis (1)
Dr. T. Y. Wu (1)
T. Kiceniuk (1)
Library (1)
- 1 Hydronautics, Inc., Rockville, Md.
- 1 Illinois Institute of Technology, Chicago (Head, Department of
Mechanical Engineering)
- 1 Institute of Aerospace Sciences, Inc., New York City (Librarian)
- 1 Johns Hopkins University, Baltimore (Head, Department of Mechan-
ical Engineering)
- 1 Lehigh University, Bethlehem, Pa. (Civil Engineering Department)
- 1 Lockheed Aircraft Corporation, Burbank, Calif. (Library)
- ① Lockheed Aircraft Corporation, Missiles and Space Division, Palo
Alto, Calif. (R. W. Kermeen)
- ② Massachusetts Institute of Technology, Cambridge
Department of Civil Engineering (1)
Department of Naval Architecture and Marine Engineering (1)
- 1 McDonnell Aircraft Corporation, St. Louis (Library)
- 1 Mississippi State University, State College (Aerophysics Department)
- 1 New York State Maritime College, Fort Schuyler (Librarian)
- 1 New York University, Institute of Mathematical Science, New York
City
- ① North American Aviation, Inc., Los Angeles (Technical Library,
Department 56)
- ① Oceanics Incorporated, New York City
- 1 Operations Research, Inc., Los Angeles

ABSTRACT CARD

U. S. Naval Ordnance Test Station

Free-Surface Water-Tunnel Tests of an Uncam-
bered Base-Vented Parabolic Hydrofoil of Aspect
Ratio One, by Thomas G. Lang and Dorothy A.
Daybell. China Lake, Calif., NOTS, Septem-
ber 1962. 36 pp. (NAVWEPS Report 7920, NOTS
TP 2942), UNCLASSIFIED.



(Over)
2 cards, 4 copies

U. S. Naval Ordnance Test Station

Free-Surface Water-Tunnel Tests of an Uncam-
bered Base-Vented Parabolic Hydrofoil of Aspect
Ratio One, by Thomas G. Lang and Dorothy A.
Daybell. China Lake, Calif., NOTS, Septem-
ber 1962. 36 pp. (NAVWEPS Report 7920, NOTS
TP 2942), UNCLASSIFIED.



(Over)
2 cards, 4 copies

U. S. Naval Ordnance Test Station

Free-Surface Water-Tunnel Tests of an Uncam-
bered Base-Vented Parabolic Hydrofoil of Aspect
Ratio One, by Thomas G. Lang and Dorothy A.
Daybell. China Lake, Calif., NOTS, Septem-
ber 1962. 36 pp. (NAVWEPS Report 7920, NOTS
TP 2942), UNCLASSIFIED.



(Over)
2 cards, 4 copies

U. S. Naval Ordnance Test Station

Free-Surface Water-Tunnel Tests of an Uncam-
bered Base-Vented Parabolic Hydrofoil of Aspect
Ratio One, by Thomas G. Lang and Dorothy A.
Daybell. China Lake, Calif., NOTS, Septem-
ber 1962. 36 pp. (NAVWEPS Report 7920, NOTS
TP 2942), UNCLASSIFIED.



(Over)
2 cards, 4 copies

NAWWEPS Report 7920

ABSTRACT. Results of water-tunnel tests on the base-vented hydrofoil model show that the lift and moment coefficients and the lift coefficient derivative are all essentially independent of ventilation number and are approximately equal to coefficients of uncambered airfoils having the same aspect ratio.

The drag coefficient agreed only partially with two-dimensional cavity drag theory. The maximum lift-to-drag ratio was 6.5 when fully vented and 2.4 when fully wetted.

(Contd. on Card 2)

NAWWEPS Report 7920

ABSTRACT. Results of water-tunnel tests on the base-vented hydrofoil model show that the lift and moment coefficients and the lift coefficient derivative are all essentially independent of ventilation number and are approximately equal to coefficients of uncambered airfoils having the same aspect ratio.

The drag coefficient agreed only partially with two-dimensional cavity drag theory. The maximum lift-to-drag ratio was 6.5 when fully vented and 2.4 when fully wetted.

(Contd. on Card 2)

NAWWEPS Report 7920

ABSTRACT. Results of water-tunnel tests on the base-vented hydrofoil model show that the lift and moment coefficients and the lift coefficient derivative are all essentially independent of ventilation number and are approximately equal to coefficients of uncambered airfoils having the same aspect ratio.

The drag coefficient agreed only partially with two-dimensional cavity drag theory. The maximum lift-to-drag ratio was 6.5 when fully vented and 2.4 when fully wetted.

(Contd. on Card 2)

NAWWEPS Report 7920

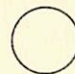
ABSTRACT. Results of water-tunnel tests on the base-vented hydrofoil model show that the lift and moment coefficients and the lift coefficient derivative are all essentially independent of ventilation number and are approximately equal to coefficients of uncambered airfoils having the same aspect ratio.

The drag coefficient agreed only partially with two-dimensional cavity drag theory. The maximum lift-to-drag ratio was 6.5 when fully vented and 2.4 when fully wetted.


(Contd. on Card 2)

ABSTRACT CARD

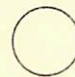
U. S. Naval Ordnance Test Station
Free-Surface Water-Tunnel . . . (Card 2)
Due to the reduced blockage of the Free-Surface Water Tunnel at the California Institute of Technology, the minimum ventilation number (K) was 0.02 and the minimum air-flow rate coefficient (Q'_{cr}) providing full ventilation was 0.026 (rate increasing) and 0.013 (rate decreasing).

 NAVWEPS Report 7920

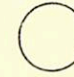
U. S. Naval Ordnance Test Station
Free-Surface Water-Tunnel . . . (Card 2)
Due to the reduced blockage of the Free-Surface Water Tunnel at the California Institute of Technology, the minimum ventilation number (K) was 0.02 and the minimum air-flow rate coefficient (Q'_{cr}) providing full ventilation was 0.026 (rate increasing) and 0.013 (rate decreasing).

 NAVWEPS Report 7920

U. S. Naval Ordnance Test Station
Free-Surface Water-Tunnel . . . (Card 2)
Due to the reduced blockage of the Free-Surface Water Tunnel at the California Institute of Technology, the minimum ventilation number (K) was 0.02 and the minimum air-flow rate coefficient (Q'_{cr}) providing full ventilation was 0.026 (rate increasing) and 0.013 (rate decreasing).

 NAVWEPS Report 7920

U. S. Naval Ordnance Test Station
Free-Surface Water-Tunnel . . . (Card 2)
Due to the reduced blockage of the Free-Surface Water Tunnel at the California Institute of Technology, the minimum ventilation number (K) was 0.02 and the minimum air-flow rate coefficient (Q'_{cr}) providing full ventilation was 0.026 (rate increasing) and 0.013 (rate decreasing).

 NAVWEPS Report 7920

- 2 Ordnance Research Laboratory, Pennsylvania State University,
University Park (Garfield Thomas Water Tunnel)
- 1 Pacific Aeronautical Library of the IAS, Los Angeles
- 1 Reed Research, Inc.
- 1 Rensselaer Polytechnic Institute, Troy, N. Y. (Department of Mathematics)
- 1 Republic Aviation Corporation, Farmingdale, N. Y.
- 1 Rocketdyne, Canoga Park, Calif. (Library, Department 596-6)
- 1 Rose Polytechnic Institute, Terre Haute, Ind. (Library)
- 1 Society of Naval Architects and Marine Engineers, New York City
- 2 Southwest Research Institute, San Antonio
Director, Department of Applied Mechanics (1)
Editor, Applied Mechanics Review (1)
- 1 Stanford University, Stanford, Calif. (Department of Civil Engineering, Prof. B. Perry)
- 1 Technical Research Group, Syosset, N. Y.
- 1 The Boeing Company, Seattle (Library, Organization No. 2-5190)
- 2 The Martin Company, Baltimore (Science Technical Library)
- 1 The Rand Corporation, Santa Monica, Calif. (Technical Library)
- 4 The University of Michigan, Ann Arbor
Department of Civil Engineering (1)
Department of Engineering Mechanics (1)
Department of Naval Architecture and Marine Engineering (2)
- 1 The University of Southern California, Los Angeles (Engineering Center)
- 1 Thompson Ramo Wooldridge, Inc., Cleveland (Chief Engineering Science Group)
- 1 United Technology Corporation, Sunnyvale, Calif. (Technical Library)
- 2 University of California, College of Engineering, Berkeley
Prof. J. V. Wehausen (1)
Library (1)
- 1 University of Illinois, Urbana (College of Engineering)
- 2 University of Iowa, Iowa Institute of Hydraulic Research, Iowa City
Prof. H. Rouse (1)
Prof. L. Landweber (1)
- 1 University of Kansas, School of Architecture and Engineering, Lawrence
- 1 University of Maryland, Institute of Fluid Dynamics and Applied Mathematics, College Park
- 1 University of Minnesota, St. Anthony Falls Hydraulic Laboratory, Minneapolis
- 1 University of Nebraska, Lincoln (Department of Engineering Mechanics)
- 1 University of Notre Dame (Department of Engineering Mechanics)
- 1 University of Wisconsin, Mathematics Research Center, Madison (Prof. L. M. Milne-Thomson)
- 1 Vitro Corporation of America, Silver Spring Laboratory (Librarian)
- 1 Vought Aeronautics, Dallas (Engineering Library)
- 1 Webb Institute of Naval Architecture, Glen Cove, N. Y. (Technical Library)

- 1 Westinghouse Electric Corporation, Baltimore (Engineering Librarian)
- 1 Westinghouse Electric Corporation, Sunnyvale, Calif. (Library)
- 1 Westinghouse Research Laboratories, Pittsburgh (Library)
- 1 Woods Hole Oceanographic Institution, Woods Hole, Mass.